Accepted Manuscript

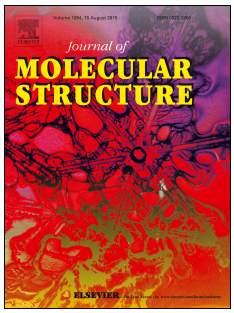

Synthesis, spectroscopic investigations, DFT studies, molecular docking and antimicrobial potential of certain new indole-isatin molecular hybrids: Experimental and theoretical approaches

Maha S. Almutairi, Azza S. Zakaria, P. Primsa Ignasius, Reem I. Al-Wabli, Isaac Hubert Joe, Mohamed I. Attia

PII: S0022-2860(17)31356-X

DOI: 10.1016/j.molstruc.2017.10.025

Reference: MOLSTR 24396

To appear in: *Journal of Molecular Structure*

Received Date: 24 July 2017

Revised Date: 4 October 2017

Accepted Date: 6 October 2017

Please cite this article as: M.S. Almutairi, A.S. Zakaria, P.P. Ignasius, R.I. Al-Wabli, I.H. Joe, M.I. Attia, Synthesis, spectroscopic investigations, DFT studies, molecular docking and antimicrobial potential of certain new indole-isatin molecular hybrids: Experimental and theoretical approaches, *Journal of Molecular Structure* (2017), doi: 10.1016/j.molstruc.2017.10.025.

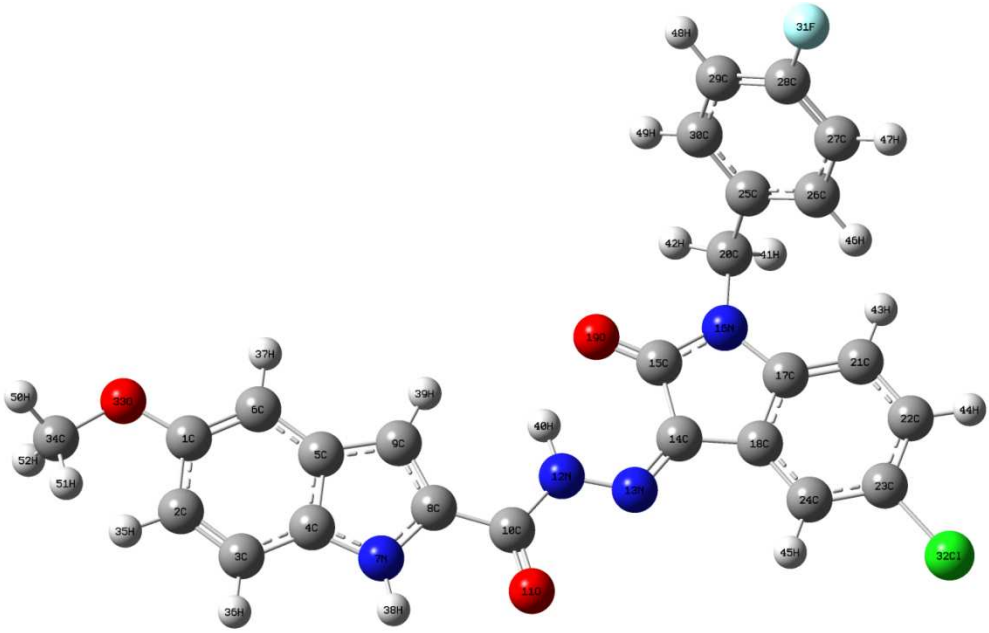

Synthesis, spectroscopic investigations, DFT studies, molecular docking and antimicrobial potential of certain new indole-isatin molecular hybrids: Experimental and theoretical approaches

Maha S. Almutairi[a], Azza S. Zakaria[b], P. Primsa Ignasius[c,d], Reem I. Al-Wabli[a], Isaac Hubert Joe[c] and Mohamed I. Attia[a,e*]

[a]Department of Pharmaceutical Chemistry, College of Pharmacy, King Saud University, Riyadh 11451, Saudi Arabia
[b]Department of Microbiology and Immunology, Faculty of Pharmacy, Alexandria University, 21521 Alexandria, Egypt
[c]Centre for Molecular and Biophysics Research, Mar Ivanios College, Thiruvananthapuram 695015, Kerala, India.
[d]Department of Physics, Government College, Nedumangad, Thiruvananthapuram 695541, Kerala, India
[e]Medicinal and Pharmaceutical Chemistry Department, Pharmaceutical and Drug Industries Research Division, National Research Centre (ID: 60014618), El Bohooth Street, Dokki, Giza 12622, Egypt

Keywords: 5-Methoxyindole; Isatin, FT-IR; FT-Raman; DFT; Antimicrobial

Abstract

Indole-isatin molecular hybrids **5a-i** have been synthesized and characterized by different spectroscopic methods to be evaluated as new antimicrobial agents against a panel of Gram positive bacteria, Gram negative bacteria, and moulds. Compound **5h** was selected as a representative example of the prepared compounds **5a-i** to perform computational investigations. Its vibrational properties have been studied using FT-IR and FT-Raman with the aid of density functional theory (DFT) approach. The natural bond orbital (NBO) analysis as well as HOMO and LUMO molecular orbitals investigations of compound **5h** were carried out to explore its possible intermolecular delocalization or hyper-conjugation and its possible interactions with the target protein. Molecular docking of compound **5h** predicted its binding mode with the fungal target protein.

1. Introduction

Indole (benzopyrrole) is an aromatic bicyclic structure consisting of fused benzene and pyrrole rings through the 2- and 3-positions of the pyrrole fragment. Since its first synthesis in 1866, indole was found in many natural products like fungal metabolities, vinca alkaloids, and marine natural products in addition to its incorporation in various bioactive agrochemicals and pharmaceuticals [1, 2]. In the last few years it has been documented that indole myriad derivatives and its bioisosters have a wide spectrum of bioactivities ranging from antimicrobial to anticancer activities [2-5]. Moreover, 5-methoxyindole constitutes the scaffold of the natural hormone melatonin (MLT). MLT and its derivatives have diverse pharmaceutical applications such as treatment of depression, headache, sleep disorders, and as anticancer agents [6-8].

On the other hand, 2,3-dioxindole (isatin) is an oxidised form of indole and it has been identified as an endogenous molecule in humans and other mammals [9]. It contains different functionalizable groups and it possesses privileged electronic characteristics with unique molecular size giving it the ability to exhibit diverse beneficial biological properties. Isatin constitutes the backbone of a relatively large number of bioactive compounds endowed with various useful biological activities such as antibacterial [10, 11], antifungal [12], anticonvulsant [13], and anticancer activities [14-16]. Consequently, isatin-bearing compounds have captured the attention in different research fields particularly in the medical research area.

Molecular hybridization is a well known strategy in medicinal chemistry to get new potent bioactive molecules [17, 18]. Therefore, the molecular hybrids **5a-i** incorporating both isatin and 5-methoxyindole moieties were designed and synthesized to be evaluated as new

antimicrobial agents. Single crystal X-ray structure of compound **5h**, as a representative example of the synthesized compounds **5a-i**, confirmed their imine double bond configuration. In addition, the vibrational properties of compound **5h** have been investigated in the current study using FT-IR and FT-Raman characterizations aided by density functional theory (DFT) computations in order to gain insight into its inter- and intra-molecular interactions as well as the equilibrium structural geometry of this type of compounds. Whilst, the natural bond orbital (NBO) analysis of compound **5h** has been performed to determine its possible intermolecular delocalization or hyper-conjugation. Also, compound **5h** was subjected to HOMO and LUMO molecular orbitals investigations to explore its possible interactions with the target protein. Molecular docking studies predicted the binding mode of compound **5h** with its target protein.

2. Experimental details

2.1. General

The melting points were measured using a Gallenkamp melting point device and are uncorrected. The FT-IR spectrum of compound **5h** was recorded using Perkin-Elmer RXL spectrometer (Waltham, Massachusetts, USA) in the region 4000-500 cm^{-1}, with samples in the KBr pellet method with resolution of 2 cm^{-1}. The Raman spectrum of compound **5h** was recorded in the region 3500-50 cm^{-1} using Bruker RFS-27 spectrophotometer (Ettlingen, Germany) having resolution of 2 cm^{-1}. The NMR samples of the synthesized compounds **5a-i** were dissolved in DMSO-d_6 and the NMR spectra were recorded using Bruker NMR spectrometer (Bruker, Reinstetten, Germany) at 500 MHz for ^{1}H and 125.76 MHz for ^{13}C at the Research Center, College of Pharmacy, King Saud University, Saudi Arabia. Chemical shifts are expressed in δ-values (ppm) relative to TMS as an internal standard. Elemental analyses were carried out at Microanalysis Laboratory, Cairo University, Cairo, Egypt and the results agreed favorably with the proposed structures within ± 0.4 % of the theoretical values. Mass spectra were recorded using Agilent Quadrupole 6120 LC/MS with ESI (Electrospray ionization) source (Agilent Technologies, Palo Alto, CA, USA). Synthesis of compounds **4a-i** has been previously reported [19-21].

2.2. Synthesis

2.2.1. Synthesis of methyl 5-methoxy-1H-indole-2-carboxylate (**2**)

Compound **2** was prepared according to the literature procedure and its spectral data were consistent with the published ones [22].

2.2.2. Synthesis of 5-methoxy-1H-indole-2-carbohydrazide (**3**)

Hydrazine hydrate (0.32 g, 10 mmol) was added to a suspension of compound **2** (0.21 g, 1 mmol) in methanol (15 mL). The reaction mixture was heated under reflux for three hours, cooled to room temperature and filtered. The collected solid was dried to give 0.19 g (90%) of the carbohydrazide derivative **3** [23] as a white powder m.p. 266-268 °C which was pure enough to be used in the subsequent reactions.

2.2.3. General procedure for the synthesis of target compounds **5a-i**

A mixture of compound **3** (1 mmol) and the appropriate isatin derivative **4a-i** (1 mmol) in absolute ethyl alcohol and catalytic amount of glacial acetic acid was heated under reflux for 4 h, filtered while hot and the collected solid was washed with ethanol. The crude products **5a-i** were re-crystallized from ethanol/DMF mixture (3:1) to furnish the pure title compounds **5a-i** in 43-94% yields.

2.2.3.1. 5-Methoxy-N'-[(3Z)-1-methyl-2-oxo-1,2-dihydro-3H-indol-3-ylidene]-1H-indole-2-carbohydrazide (**5a**): Yellow powder m.p. > 300 °C (yield 55%); ^{1}H NMR (DMSO-d_6) *ppm*: 3.23 (s, 3H, NCH_3), 3.79 (s, 3H, OCH_3), 6.93 (s, 1H, $H_{ar.}$), 7.13-7.18 (m, 3H, $H_{ar.}$), 7.22 (s, 1H, $H_{ar.}$), 7.39-7.49 (m, 2H, $H_{ar.}$), 8.09 (s, 1H, $H_{ar.}$), 11.71 (s, 1H, NH), 11.85 (s, 1H, NH); ^{13}C NMR (DMSO-d_6) *ppm*: 26.5 (NCH_3), 55.7 (OCH_3), 102.6, 109.8, 112.4, 113.9, 115.4, 116.7, 122.8, 126.8, 127.8, 129.2, 129.5, 133.1, 139.8, 145.4, 154.5 ($C_{ar.}$, $CH_{ar.}$, C=N), 161.5, 163.9 (2 x C=O); MS *m/z*: 349 $[M+1]^+$.

2.2.3.2. N'-[(3Z)-5-Bromo-1-methyl-2-oxo-1,2-dihydro-3H-indol-3-ylidene]-5-methoxy-1H-indole-2-carbohydrazide (**5b**): Orange powder m.p. > 300 °C (yield 71%); ^{1}H NMR (DMSO-d_6) *ppm*: 3.21 (s, 3H, NCH_3), 3.79 (s, 3H, OCH_3), 6.94 (dd, *J* = 8.5, 2.0 Hz, 1H, $H_{ar.}$), 7.09 (d, *J* = 8.5 Hz, 1H, $H_{ar.}$), 7.18 (d, *J* = 1.5 Hz, 1H, $H_{ar.}$), 7.39 (d, *J* = 8.5 Hz, 1H, $H_{ar.}$), 7.57 (s, 1H, $H_{ar.}$), 7.67 (dd, *J* = 8.0, 0.5 Hz, 1H, $H_{ar.}$), 8.36 (s, 1H, $H_{ar.}$), 11.83 (s, 1H, NH), 11.89 (s, 1H, NH); ^{13}C NMR (DMSO-d_6) *ppm*: 26.6 (NCH_3), 55.8 (OCH_3), 102.6, 111.6, 113.9, 114.5, 115.5, 116.9, 117.0, 121.7, 123.2, 127.8, 128.9, 132.5, 134.9, 144.5, 154.5 ($C_{ar.}$, $CH_{ar.}$, C=N), 160.4, 163.9 (2 x C=O); MS *m/z*: 428 $[M+1]^+$.

2.2.3.3. N'-[(3Z)-5-Chloro-1-methyl-2-oxo-1,2-dihydro-3H-indol-3-ylidene]-5-methoxy-1H-indole-2-carbohydrazide (**5c**): Yellow powder m.p. > 300 °C (yield 43%); ^{1}H NMR (DMSO-d_6) *ppm*: 3.22 (s, 3H, NCH_3), 3.79 (s, 3H, OCH_3), 6.94 (dd, *J* = 8.5, 2.0 Hz, 1H, $H_{ar.}$), 7.14 (d, *J* = 8.5 Hz, 1H, $H_{ar.}$), 7.18 (d, *J* = 2.0 Hz, 1H, $H_{ar.}$), 7.39 (d, *J* = 8.5 Hz, 1H, $H_{ar.}$), 7.55 (dd, *J* = 8.5, 1.5 Hz, 1H, $H_{ar.}$), 7.56 (s, 1H, $H_{ar.}$), 8.24 (s, 1H, $H_{ar.}$), 11.83 (s, 1H, NH), 11.88 (s, 1H, NH); ^{13}C NMR (DMSO-d_6) *ppm*: 26.7 (NCH_3), 55.8 (OCH_3), 102.6, 111.1, 113.9, 116.4,

116.9, 120.5, 126.3, 126.8, 127.8, 129.2, 131.2, 132.2, 133.0, 144.1, 154.5 ($C_{ar.}$, $CH_{ar.,}$ C=N), 159.9, 163.8 (2 x C=O); MS *m/z*: 384 $[M+1]^+$.

2.2.3.4. N'-[(3Z)-5-Fluoro-1-methyl-2-oxo-1,2-dihydro-3H-indol-3-ylidene]-5-methoxy-1H-indole-2-carbohydrazide (**5d**): Yellow powder m.p. > 300 °C (yield 71%); ^{1}H NMR (DMSO-d_6) *ppm*: 3.22 (s, 3H, NCH_3), 3.79 (s, 3H, OCH_3), 6.94-6.96 (m, 1H, $H_{ar.}$), 7.12-7.15 (m, 1H, $H_{ar.}$), 7.19 (d, *J* = 2.0 Hz, 1H, $H_{ar.}$), 7.36-7.40 (m, 2H, $H_{ar.}$), 7.57 (s, 1H, $H_{ar.}$), 8.05 (d, *J* = 8.0 Hz, 1H, $H_{ar.}$), 11.82 (s, 1H, NH), 11.84 (s, 1H, NH); ^{13}C NMR (DMSO-d_6) *ppm*: 26.7 (NCH_3), 55.8 (OCH_3), 102.6, 113.9, 116.9, 127.8, 129.2, 133.1, 138.0, 141.7, 154.5 ($C_{ar.}$, $CH_{ar.,}$ C=N), 110.6 ($C_{3'\text{-}F}$, *J* = 8.0 Hz, $C_{ar.}$), 114.1 ($C_{2'\text{-}F}$, *J* = 26.4 Hz, $C_{ar.}$), 115.8 ($C_{3'\text{-}F}$, *J* = 9.0 Hz, $C_{ar.}$), 118.9 ($C_{2'\text{-}F}$, *J* = 23.1 Hz, $C_{ar.}$), 129.2 ($C_{4'\text{-}F}$, *J* = 3.0 Hz, $C_{ar.}$), 158.3 ($C_{1'\text{-}F}$, *J* = 235.4 Hz, $C_{ar.}$) 161.7, 163.9 (2 x C=O); MS *m/z*: 367 $[M+1]^+$.

2.2.3.5. 5-Methoxy-N'-[(3Z)-5-methoxy-1-methyl-2-oxo-1,2-dihydro-3H-indol-3-ylidene]-1H-indole-2-carbohydrazide (**5e**): Orange powder m.p. > 300 °C (yield 94%); ^{1}H NMR (DMSO-d_6) *ppm*: 3.20 (s, 3H, NCH_3), 3.79 (s, 3H, OCH_3), 3.84 (s, 3H, OCH_3), 6.92-6.95 (m, 1H, $H_{ar.}$), 7.09-7.12 (m, 2H, $H_{ar.}$), 7.23 (d, *J* = 1.5 Hz, 1H, $H_{ar.}$), 7.38 (d, *J* = 9.0 Hz, 1H, $H_{ar.}$), 7.53 (s, 1H, $H_{ar.}$), 7.74 (s, 1H, $H_{ar.}$), 11.82 (s, 1H, NH), 12.02 (s, 1H, NH); ^{13}C NMR (DMSO-d_6) *ppm*: 26.6 (NCH_3), 55.7 (OCH_3), 56.4 (OCH_3), 102.6, 110.2, 111.4, 113.3, 115.9, 116.9, 120.4, 127.8, 128.6, 129.5, 132.9, 137.8, 140.8, 154.5, 154.7 ($C_{ar.}$, $CH_{ar.,}$ C=N), 160.8, 162.5 (2 x C=O); MS *m/z*: 379 $[M+1]^+$.

2.2.3.6. N'-[(3Z)-1-(4-Fluorobenzyl)-2-oxo-1,2-dihydro-3H-indol-3-ylidene]-5-methoxy-1H-indole-2-carbohydrazide (**5f**): Yellow powder m.p. 258-260 °C (yield 84%); ^{1}H NMR (DMSO-d_6) *ppm*: 3.79 (s, 3H, OCH_3), 5.01 (s, 2H, CH_2), 6.94-6.95 (m, 1H, $H_{ar.}$), 7.09 (d, *J* = 8.0 Hz, 1H, $H_{ar.}$), 7.18-7.21 (m, 4H, $H_{ar.}$), 7.39-7.46 (m, 4H, $H_{ar.}$), 7.56 (s, 1H, $H_{ar.}$), 8.12 (d, *J* = 7.5 Hz, 1H, $H_{ar.}$), 11.74 (s, 1H, NH), 11.86 (s, 1H, NH); ^{13}C NMR (DMSO-d_6) *ppm*: 42.5 (CH_2), 55.7 (OCH_3), 102.6, 110.3, 113.9, 116.8, 121.2, 123.1, 127.0, 127.8, 129.8, 129.9, 132.9, 133.1, 142,9, 144.1, 154.5 ($C_{ar.}$ and $CH_{ar.}$, C=N), 115.9 ($C_{2',6'\text{-}F}$, *J* = 21.4 Hz, $C_{ar.}$), 130.1 ($C_{3',5'\text{-}F}$, *J* = 8.1 Hz, $C_{ar.}$), 132.4 ($C_{4'\text{-}F}$, *J* = 2.0 Hz, $C_{ar.}$), 161.9 ($C_{1'\text{-}F}$, *J* = 241.9 Hz, $C_{ar.}$), 163.1, 164.1 (2 x C=O); MS *m/z*: 443 $[M+1]^+$.

2.2.3.7. N'-[(3Z)-5-Bromo-1-(4-fluorobenzyl)-2-oxo-1,2-dihydro-3H-indol-3-ylidene]-5-methoxy-1H-indole-2-carbohydrazide (**5g**): Yellow powder m.p. 238-240 °C (yield 60%); ^{1}H NMR (DMSO-d_6) *ppm*: 3.79 (s, 3H, OCH_3), 5.04 (s, 2H, CH_2), 6.97-7.88 (m, 11H, $H_{ar.}$), 12.07 (s, 1H, NH), 13.82 (s, 1H, NH); ^{13}C NMR (DMSO-d_6) *ppm*: 42.5 (CH_2), 55.8 (OCH_3), 102.7, 110.9, 112.9, 113.9, 115.8, 115.9, 116.1, 117.2, 122.1, 123.5, 127.8, 130.1, 130.2,

132.1, 133.5, 134,1, 141.9, 154.7, 161.4 ($C_{ar.}$ and $CH_{ar.}$, C=N), 161.8, 162.8 (2 x C=O), MS *m/z*: 522 $[M+1]^+$.

2.2.3.8. N'-[(3Z)-5-Chloro-1-(4-fluorobenzyl)-2-oxo-1,2-dihydro-3H-indol-3-ylidene]-5-methoxy-1H-indole-2-carbohydrazide (**5h**): Orange powder m.p. 250-252 °C (yield 59%); ^{1}H NMR (DMSO-d_6) *ppm*: 3.79 (s, 3H, OCH_3), 5.00 (s, 2H, CH_2), 6.83 (d, *J* = 8.5 Hz, 1H, $H_{ar.}$), 6.95-6.98 (m, 1H, $H_{ar.}$), 7.12-7.25 (m, 4H, $H_{ar.}$), 7.35-7.51 (m, 3H, $H_{ar.}$), 7.73 (s, 1H, $H_{ar.}$), 8.52 (s, 1H, $H_{ar.}$), 11.37 (s, 1H, NH), 12.04 (s, 1H, NH); ^{13}C NMR (DMSO-d_6) *ppm*: 42.2 (CH_2), 55.8 (OCH_3), 102.5, 111.5, 112.5, 113.5, 115.8, 115.9, 116.1, 117.5, 121.7, 121.9, 128.2, 129.7, 129.8, 130.1, 130.2, 132,1, 140.5, 154.9, 162.5 ($C_{ar.}$ and $CH_{ar.}$, C=N), 162.6, 163.1 (2 x C=O); MS *m/z*: 478 $[M+1]^+$.

2.2.3.9. N'-[(3Z)-5-Fluoro-1-(4-fluorobenzyl)-2-oxo-1,2-dihydro-3H-indol-3-ylidene]-5-methoxy-1H-indole-2-carbohydrazide (**5i**): Yellow powder m.p. 258-260 °C (yield 68%); ^{1}H NMR (DMSO-d_6) *ppm*: 3.79 (s, 3H, OCH_3), 5.04 (s, 2H, CH_2), 6.95 (dd, *J* = 2.0, 9.0 Hz, 1H, H_{ar}), 7.07-7.09 (m, 2H, $H_{ar.}$), 7.17-7.21 (m, 4H, $H_{ar.}$), 7.41 (d, *J* = 9.0 Hz, 1H, $H_{ar.}$), 7.42-7.45 (m, 2H, $H_{ar.}$), 7.49-7.51 (m, 1H, $H_{ar.}$), 8.11 (d, *J* = 8.0 Hz, 1H, $H_{ar.}$), 11.85 (s, 2H, 2 x NH); ^{13}C NMR (DMSO-d_6) *ppm*: 43.1 (CH_2), 55.7 (OCH_3), 102.7, 111.0, 111.1, 113.9, 116.5, 116.9, 117.2, 120.8, 121.3, 127.9, 129.8, 129.9, 133,1, 140.4, 154.5 ($C_{ar.}$ and $CH_{ar.}$, C=N), 116.0 ($C_{2',6'-F}$, *J* = 21.3 Hz, $C_{ar.}$), 130.2 ($C_{3',5'-F}$, *J* = 8.1 Hz, $C_{ar.}$), 132.8 ($C_{4'-F}$, *J* = 2.6 Hz, $C_{ar.}$), 158.4 ($C_{1'-F}$, *J* = 236.0 Hz, $C_{ar.}$), 161.1, 162.9 (2 x C=O); MS *m/z*: 461 $[M+1]^+$.

2.3. Antimicrobial evaluation

2.3.1. Antimicrobial agents

Ampicillin (AMP) was purchased from Sigma-Aldrich Co. (St. Louis, MO, USA) and fluconazole (FLC) from Shouguang-Fukang Pharmaceutical Ltd. (Shandong, China). AMP was used as positive control for bacteria while FLC was used as positive control for fungi. The antimicrobial discs (containing 10 µg AMP or 25 µg FLC) were purchased from ROSCO (Neo-Sensitabs, Taastrup, Denmark). 100% Dimethyl sulfoxide (DMSO) was used to dissolve FLC and/or the tested compounds **5a-i** to obtain an initial concentration of 1000 µg/mL. These stock solutions were then diluted to the desired concentrations with sterile distilled water. AMP was dissolved in water to obtain an initial concentration of 1000 µg/mL. AMP and FLC antifungal discs were stored at -80°C until used.

2.3.2. Media

Muller Hinton broth (MHB) and Muller Hinton agar (MHA) were purchased from Sigma-Aldrich Co. (St. Louis, MO, USA) and were used for the antimicrobial assay of the bacterial isolates. Liquid RPMI 1640 medi um supplemented with L-glutamine was purchased from

Sigma-Aldrich Co. (St. Louis, MO, USA) and was added to 2% sodium bicarbonate and 0.165 M 3-morpholinepropanesulfonic acid (MOPS) from Dojindo Laboratories (Kumamoto, Japan) then adjusted to pH 7.0 and was used for the assay of the yeast and moulds. Nutrient agar, MacConkey's agar, mannitol salt agar, cetrimide agar, sabouraud dextrose agar (SDA) and Brain heart infusion broth (BHI) from Difco Laboratories (Detroit, MI, USA). Potato dextrose agar (PDA) was purchased from Eiken Chemical Co. Ltd. (Tokyo, Japan).

2.3.3. Organisms

Five Gram negative organisms, namely *Escherichia coli* (*E. coli*), *Pseudomonas aeruginosa* (*Ps. aeruginosa*), *Proteus vulgaris* (*p. vulgaris*), *Klebsiella pneumonia* (*K. pneumonia*) and *Salmonella enteridis* (*S. enteridis*), four Gram positive isolates, namely *Staphylococcus aureus* (*S. aureus*), Methicillin resistant *Staphylococcus aureus* (MRSA), *Enterococcus fecalis* (*E. fecalis*) and *Bacillus subtilis* (*B. subtilis*) and three fungal isolates; one *Candida albicans* (*C. albicans*) and two mould isolates, *Asperagillus niger* (*A. niger*) and *Penicillum notatum* (*P. notatum*). All isolates were obtained from King Khaled Hospital, Riyadh, Saudi Arabia.

2.3.4. Culture conditions

All clinical samples were first inoculated onto Sheep blood agar (SPML Co. Ltd, Riyadh, Saudi Arabia), The plates were incubated at 37 °C for 24-48 h. Identification of isolates was done according to the standard methods described elsewhere [24, 25] and Clinical Laboratory Standards Institute (CLSI) [26]. Isolates were stored in BHI broth containing 16% (w/v) glycerol at −80 °C until further use.

2.3.5. Growth of the tested microorganisms

Staphylococcal isolates were re-inoculated onto mannitol salt agar and then the plates were incubated at 37 °C for 24-48 h. Mannitol fermentation was observed and recorded. Gram negative isolates were re-inoculated onto MacConkey's agar and then the plates were incubated at 37 °C for 24-48 h. Lactose fermentation was observed and recorded. *Ps. aeruginosa* strains were further re-inoculated on cetrimide agar at 37 °C for 24 h.

2.3.6. Determination of Minimum Inhibitory Concentrations (MICs)

2.3.6.1. Antibacterial susceptibility studies

Concerning the bacterial isolates (either Gram positive or Gram negative), AMP was used as a reference control. MICs of AMP and the test compounds were carried out in cation-adjusted MHB by means of microdilution broth method in accordance to National Committee for Clinical Laboratory Standards [27] and CLSI documents [28, 29] Stock solutions of AMP pure drug was prepared in sterile distilled water while stock solution of each of the test

compounds was prepared in DMSO to reach an initial concentration of 1000 mg/mL. Preparation of inocula for broth microdilution testing was carried out in accordance with CLSI standard procedures. Briefly, 0.5 McFarland equivalent inoculum of each strain was prepared in normal saline from 18-24 h agar plate culture. The suspension was further diluted to achieve desired inoculums concentration of 10^5 CFU/mL. 100 μL of aliquot of each strain were then added to a 96-well microtiter plate containing gradient concentrations of either AMP pure drug or any of the test compounds diluted in double strength MHB. The plates were then incubated at 37 °C for 24 h. The turbidity of each well was measured at 490 nm with a microplate ELISA reader. The MIC was defined as the lowest concentration of the antibiotic or the test compound that prevented bacterial growth.

2.3.6.2. Antifungal susceptibility studies

Broth microdilution testing was carried out in accordance with CLSI documents M27-A3 [30] and M38-A2 [31] with RPMI 1640 medium buffered to pH 7.0 with 0.165 M MOPS for all organisms. Stock inoculum suspensions of all yeasts were obtained from 24-h-old cultures grown on PDA at 35 °C. Stock inoculum suspensions of the filamentous fungi were prepared from cultures grown on PDA at 30 °C. The final inoculum concentrations of the yeasts and the filamentous fungi ranged from 0.65 x 10^3 to 2.5 x 10^3 CFU/mL and 0.87 x 10^4 to 3.8 x 10^4 CFU/mL, respectively. The microplates were incubated at 35 °C for 48 h. In case of yeasts, the MICs of the examined compounds and the reference control, FLC, were recorded as the lowest concentration at which 50% decrease in turbidity relative to the turbidity of the growth control was observed. Whereas, in case of the filamentous fungi, the MICs of the test compounds and FLC were recorded as the lowest concentrations at which a prominent decrease in turbidity was observed.

2.3.7. Disk diffusion assay

The disk diffusion assay was performed as described previously [32]. Colonies obtained from the bacterial or the fungal isolates under test were suspended in sterile saline and adjusted to a 0.5 McFarland standard corresponding to 5 × 10^6 CFU/mL. An aliquot of 100 µL of each isolate suspension was spread uniformly onto MHA and SDA plates for bacteria and fungi, respectively. Six mm Whatmann filter paper disks were impregnated with 1000 µg of the test compounds and were allowed to dry. Then they were placed onto the surface of the inoculated agar plates together with the standard reference discs which were then incubated at 35 °C. All tests were performed for three replicates. Plates were examined for evidence of antimicrobial activities, represented by a zone of inhibition of microorganism's growth around the holes at 24 h., and diameters of clear zones were expressed in millimetres [33].

2.3.8. Scanning electron microscopy

Overnight diluted (10^7 CFU/mL) *S. aureus* was cultured for 24 h in MHB containing **5b** sample (2X MIC). Control bacterial isolate was simultaneously done for the sake of better comparison. Primary fixation of samples was done by buffered Glutaraldehyde 2.5 % over night in refrigerator, washed by phosphate buffer (pH = 7.2) and centrifuged (3000 g, 15 min, 4 °C). Secondary fixation was done by buffered Osmium Tetroxide 1 % for one hour, then dehydration by series concentration of ethanol, embedding by resin mixture from SPI (SPI-Pon™ - Araldite® Epoxy Embedding Kit). The bacterial pellets were mounted on membrane filters (Anodisc; Whatman International Ltd, Maidstone, UK). Before examination under a scanning electron microscope (SEM, JEOL, JSM-6060 LV), specimens were coated with 100 Å of a gold-palladium mix in an ion sputter (JEOL JFC 1100) [34].

2.4. Computational methods

Geometrical parameters, atomic charges and vibrational wavenumbers have been carried out in both gas and solvent phases using Gaussian'09 program package [35] with B3LYP/6-311++G(d,p) level of basis set [36-38]. The vibrational wavenumbers were then scaled by a factor of 0.9673 to compensate the errors due to vibrational anharmonicities and the incompleteness of basis set [39]. Potential energy distribution (PED) has been conducted for the computed wavenumbers of compound **5h** using VEDA4 program [40]. Natural bond orbital analysis was performed using NBO 3.1 program [41]. The molecular docking analysis for compound **5h** was carried out using AutoDock 4.2 program [42] to find out the binding mode of compound **5h** in its target protein.

3. Results and discussion

3.1. Chemistry

Scheme 1 illustrates the synthetic pathway which was adopted to prepare the target compounds **5a-i**. The synthesis was started by esterification of the commercially available 5-methoxyindole-2-carboxylic acid (**1**) according to the literature procedure [43]. The obtained methyl ester **2** was allowed to react with hydrazine hydrate to afford the corresponding acid hydrazide **3**. Subsequently, the appropriate isatin derivative **4a-i** was reacted with compound **3** to give the respective title compounds **5a-i**.

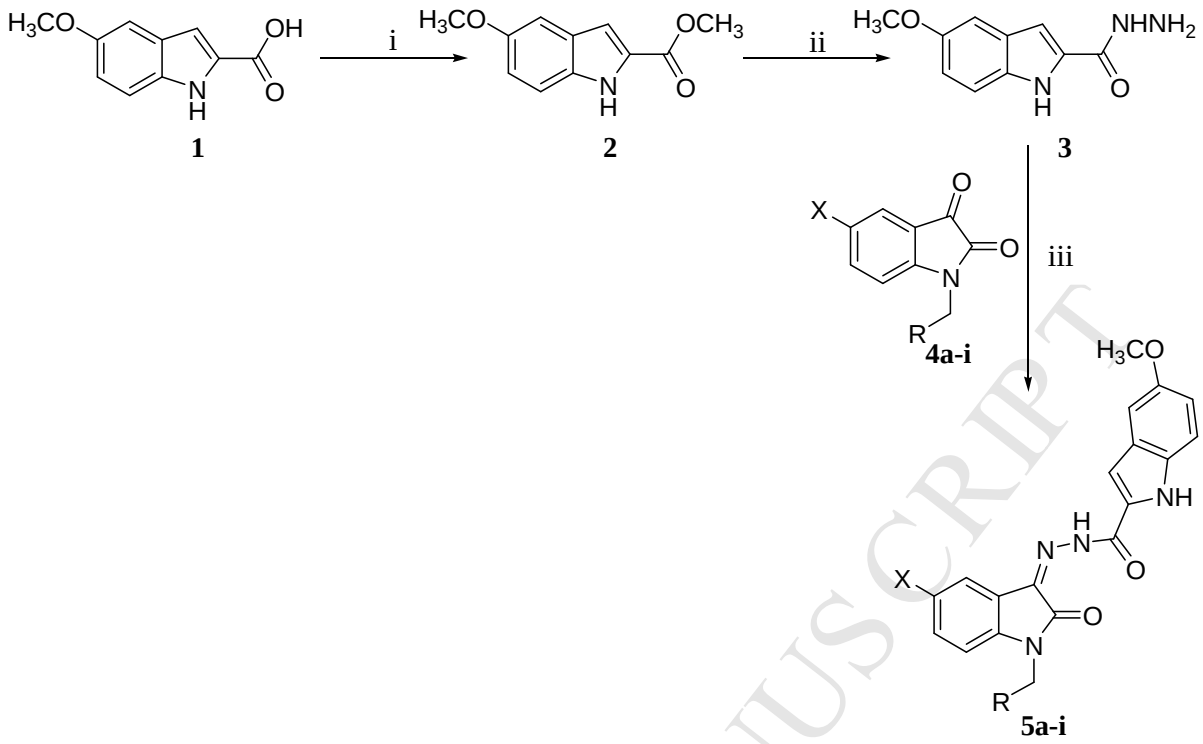

Compound No.	X	R	Compound No.	X	R
4a, 5a	H	H	**4f, 5f**	H	4-F-C_6H_4
4b, 5b	Br	H	**4g, 5g**	Br	4-F-C_6H_4
4c, 5c	Cl	H	**4h, 5h**	Cl	4-F-C_6H_4
4d, 5d	F	H	**4i, 5i**	F	4-F-C_6H_4
4e, 5e	OCH_3	H			

Scheme 1. Synthesis of the target compounds **5a-i**. *Reagents and conditions*: (i) Methanol, drops of H_2SO_4, reflux, 4 h; (ii) Methanol, H_2N-NH_2.H_2O, reflux, 2 h; (iii) Absolute ethanol, drops of acetic acid, reflux 4 h.

3.2. Antimicrobial evaluation

3.2.1. Antimicrobial spectrum

Tables 1 and 2 showed the MICs and DIZs of the test samples **5a-i**, respectively, and the reference agents against different Gram positive, Gram negative, yeasts, and filamentous fungi. Table 1 illustrates that all of the tested samples showed almost no activity against the tested Gram negative isolates as compared to the standard antimicrobial agent except toward the *Ps. aeruginosa* isolate. Most of the tested samples exhibited more Gram positive activity than Gram negative spectrum and even potent activity against a variety of fungal species. All the tested compounds showed a clear pseudomonal activity with variable MIC values of which compounds **5c** and **5d** being eight and six fold more potent than AMP, respectively.

On the other hand, none of the tested compounds showed antibacterial activity against *E. fecalis*.

All the tested compounds were highly active against the mould *P. notatum*. Although *A. niger* isolate was resistant to compounds **5c** and **5d**, it showed comparable MIC activity to that of FLC to the rest of the tested compounds and even a threefold higher activity than FLC by applying compound **5i**.

The DIZs of the tested compounds **5a-i** against the Gram-negative organisms confirmed the lack of activity of the samples against the tested isolates but for the *Ps. aeruginosa* isolate where some of the samples gave clear zones ranged from 10 to 14 mm in diameter compared to absolutely no zones with AMP. Against Gram positive organisms however, the obtained results were different, Compounds **5a**, **5b**, and **5g** showed some antibacterial activity giving a zone diameter of 22, 24, and 22 mm, respectively, though much less than that of AMP (32 mm) MD 16, 19 and 21showed some antibacterial activity giving a zone diameter of 22, 24 and 22 mm, respectively though much less than that of AMP (32 mm). Against MRSA isolate, however, many of the DIZs obtained on application of different samples produced comparable results with that of the standard antibiotic. The diameter of the inhibition zones of some of the tested compounds against either the yeast or the filamentous fungi was almost equivalent to that of FLC.

3.2.2. Scanning electron microscope

S. aureus cells were photographed by electron microscopy to compare morphological alterations after addition of compound **5b** sample to the cells with subsequent incubation for 24 h. (Figure 1). The most representative photograph was chosen even if morphologically normal organisms were also observed. Normal mounting of *S. aureus* cells under scanning electron microscope showed a clear spherical cell with grape like arrangement (Figure 1). Upon application of sample **5b** on the Gram positive cells, the obtained results showed total destruction and clumping of the bacterial cells. Abnormal forms were visible with clear change in the coccoid morphology of the bacterial cells. Some cells were shrunk while others fused together losing their normal morphology. In the mount, very few bacterial cells were found retaining their normal shape (Figure 1).

Table 1. Minimum Inhibitory Concentrations (MICs) of the title compounds **5a-i**, AMP and FLC towards Gram negative bacteria, Gram positive bacteria and fungi.

Comp. No.	MIC values (µg/mL)											
	Strain name											
	Gram negative organisms					Gram positive organisms				Fungi		
	E. coli	*Ps. aeruginosa*	*p. vulgaris*	*K. pneumonia*	*S. enteridis*	*S. aureus*	MRSA	*E. fecalis*	*B. subtilis*	*C. albicans*	*A. niger*	*P. notatum*
5a	>1000	250	500	>1000	500	15.6	15.6	500	31.3	62.5	15.6	15.6
5b	500	125	500	500	500	15.6	15.6	500	31.3	250	31.25	7.8
5c	500	3.9	500	500	500	15.6	31.3	500	31.3	62.5	500	15.6
5d	250	15.6	500	500	500	15.6	62.5	250	250	62.5	62.5	31.3
5e	250	500	250	500	500	500	500	500	500	250	15.6	250
5f	250	62.5	500	500	1000	500	500	>1000	62.5	250	31.3	15.6
5g	500	250	500	500	500	500	500	500	500	62.5	15.6	15.6
5h	500	500	500	500	500	500	500	500	250	62.5	15.6	7.8
5i	500	250	500	500	500	250	500	500	125	15.6	7.8	31.25
AMP	15.6	>1000	< 7.8	>1000	< 7.8	250	500	3.9	1000	ND	ND	ND
FLC	ND	ND	ND	ND	ND	ND	ND	ND	ND	15.6	31.3	250

ND: not determined.

Table 2. Diameter of the Inhibition Zone (DIZ) of the title compounds **5a-i**, AMP and FLC towards Gram negative bacteria, Gram positive bacteria and fungi.

Comp. No.	DIZ in mm ± S.D.*											
	Strain name											
	Gram negative organisms					Gram positive organisms				Fungi		
	E. coli	*Ps. aeruginosa*	*p. vulgaris*	*K. pneumonia*	*S. enteridis*	*S. aureus*	MRSA	*E. fecalis*	*B. subtilis*	*C. albicans*	*A. niger*	*P. notatum*
5a	12 ± 0.8	10 ± 0.8	-ve	-ve	-ve	22 ± 0.8	20 ± 0.9	-ve	14 ± 0.8	-ve	13 ± 1.0	10 ± 0.0
5b	12 ± 0.43	14 ± 2.0	-ve	-ve	10 ± 0.0	24 ± 0.43	18 ± 0.6	-ve	14 ± 0.0	-ve	-ve	14 ± 0.0
5c	10 ± 0.4	10 ± 0.9	-ve	-ve	-ve	16 ± 0.8	18 ± 0.0	-ve	18 ± 0.4	-ve	11 ± 0.0	11 ± 0.4
5d	16 ± 1.0	14 ± 2.4	-ve	-ve	-ve	18 ± 0.0	14 ± 0.5	-ve	12 ± 0.5	-ve	-ve	-ve
5e	-ve	14 ± 0.1	-ve	11 ± 0.3	11 ± 0.5	11 ± 0.7	9 ± 0.0	9 ± 0.0	11 ± 0.6	12 ± 0.8	18 ± 0.0	-ve
5f	14 ± 0.7	12 ± 0.0	-ve	12 ± 1.7	-ve	18 ± 0.0	-ve	-ve	12 ± 0.0	10±0.0	-ve	-ve
5g	18 ± 0.0	14 ± 1.6	-ve	-ve	10 ± 0.0	22 ± 1.0	-ve	12 ± 0.4	12 ± 0.7	-ve	11 ± 0.8	11 ± 1.8
5h	16 ± 0.0	10 ± 0.4	-ve	-ve	-ve	14 ± 0.4	-ve	12 ± 0.0	-ve	-ve	14 ± 1.0	10 ± 0.4
5i	14 ± 0.4	10 ± 0.0	10 ± 0.7	-ve	-ve	12 ± 0.0	-ve	12 ± 0.0	-ve	14 ± 0.3	14 ± 0.8	-ve
AMP	30 ± 0.0	-ve	36 ± 0.7	-ve	45 ± 1.0	32 ± 0.4	18 ± 0.4	35 ± 1.0	30 ± 0.5	ND	ND	ND
FLC	ND	ND	ND	ND	ND	ND	ND	ND	ND	21 ± 0.5	16 ± 0.8	15 ± 0.0

*Arithmetic mean ± standard deviation; ND: not determined.

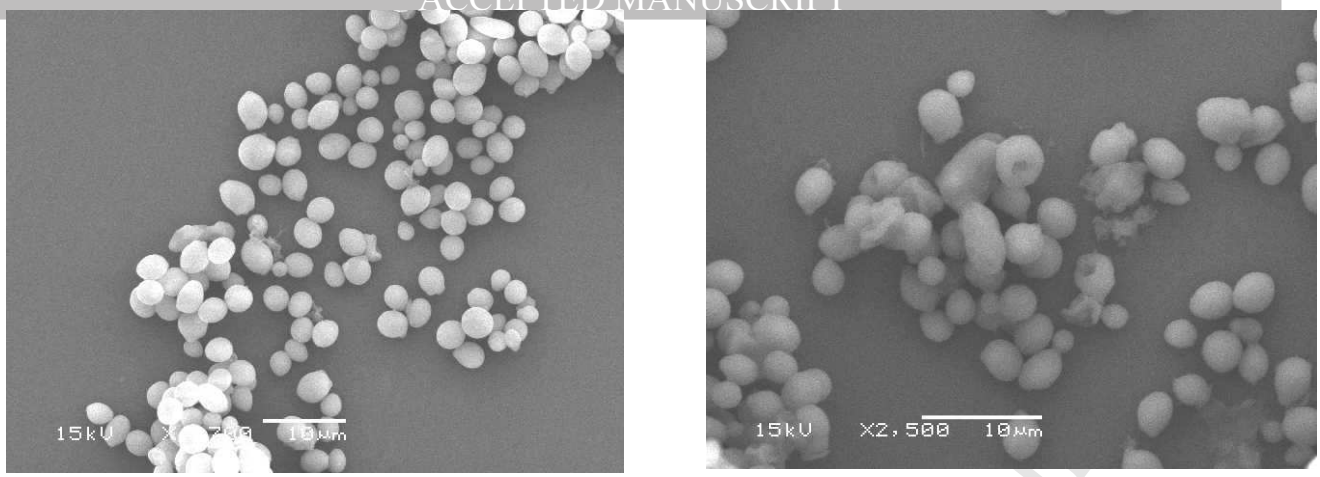

Figure 1. Scanning electron microscopy of compound **5b** after 24 h incubation with *S. aureus*.

3.3. Computational studies

3.3.1. Molecular geometry

Figure 2 illustrates the optimized structure of compound **5h**. Optimized parameters, bond lengths, bond angles and torsional angles calculated by B3LYP/6-311++G(d,p) are listed in Table 3. The global minimum energy for optimization of compound **5h** was found to be -1968.65 Hartree. The bond length C_1-C_2 in the indole ring manifested the highest value of 1.4194 and 1.4213 Å in the gas and solution phases respectively, due to its attachment to the methoxy group. The calculated bond length C_8-C_{10} in the indole ring showed good agreement with the experimental X-ray results (1.467/1.467 Å). Whereas, the bond lengths of C_{17}-N_{16}, C_{15}-N_{16}, C_{20}-N_{16}, C_8-N_7, C_4-N_7, and C_{10}-N_{12} are 1.4123, 1.3791, 1.4568, 1.3775, 1.3726, and 1.3992 Å respectively. Of all the C-N bonds C_{15}-N_{16} is comparatively higher due to the attachment of oxygen atom to the carbon atom. The bond lengths N12-H_{40} (1.0214/0.790 Å) and N_7-H_{38} (1.0092/0.847 Å) exhibited considerable deviations from the experimental X-ray data, due to the intermolecular interactions in the crystalline state. The bond angles C_3-C_4-N_7 (130.78°/130.36°), C_3-C_4-C_5 (121.48°/121.81°), C_{17}-C_{18}-C_{24} (120.72°/120.61°), N_{16}-C_{17}-C_{18} (109.74°/109.96°), and N_{16}-C_{20}-H_{41} (108.71°/109.19°) showed agreement with the experimental X-ray results, respectively. The calculated dihedral angles in solution phase of N_{13}-C_{14}-C_{15}-N_{16} and O_{33}-C_1-C_2-C_3 are 179.61 and 180.00, respectively and they are in a satisfactory agreement with the experimental XRD results. The deviations in the calculated dihedral angle values from the experimental XRD results reveal the occurrence of steric effect in the crystalline state. In general, the statistical linear regression plots between the experimental XRD values [44] and theoretical geometrical parameters showed good agreement with R^2 values in the range of 0.972-998 in the gas and solution phases (Figure

S1). The root-mean square deviation (RMSD) values were calculated for the predicted bond lengths to be 0.0300 Å (solution phase) and 0.0304 Å (gas phase) with their experimental XRD values. Similarly, the RMSD values for the predicted bond angles are 4.7308° and 7.0373° in solution and gas phases, respectively, with their XRD results. This indicates that the calculated values in solution phase are in a better agreement with the experimental values.

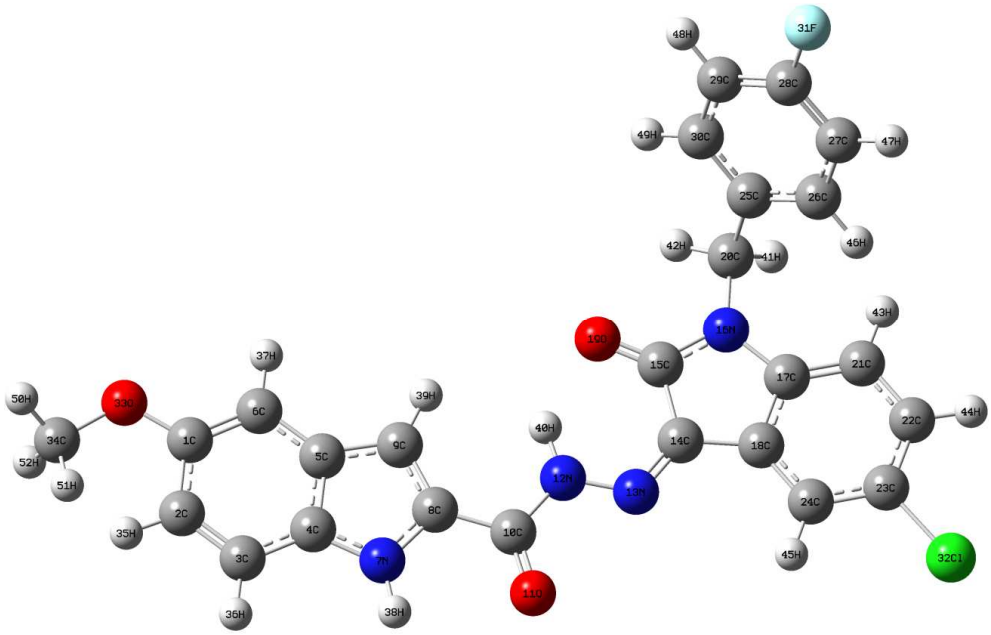

Figure 2. Optimized molecular structure of compound **5h**.

Table 3. Structural geometry parameters of compound **5h** along with the recorded XRD results.

Bond lengths (Å)				Bond Angles (°)				Dihedral angles (°)			
Parameters	Gas Phase	Solution Phase	XRD	Parameters	Gas Phase	Solution Phase	XRD	Parameters	Gas Phase	Solution Phase	XRD
C_1-C_2	1.4194	1.4213	1.414	C_2-C_1-C_6	121.07	121.10	121.46	C_6-C_1-C_2-C_3	0.003	-0.02	1.54
C_1-C_6	1.3843	1.3844	1.378	C_2-C_1-O_{33}	114.22	114.32	115.23	C_6-C_1-C_2-H_{35}	-180	179.98	-178.48
C_1-O_{33}	1.3686	1.3696	1.379	C_6-C_1-O_{33}	124.71	124.58	123.30	O_{33}-C_1-C_2-C_3	-180	-180	-179.63
C_2-C_3	1.3790	1.3797	1.385	C_1-C_2-C_3	121.57	121.68	120.60	O_{33}-C_1-C_2-H_{35}	-0.003	-0.004	0.34
C_2-H_{35}	1.0831	1.0835	0.950	C_1-C_2-H_{35}	117.62	117.88	119.63	C_2-C_1-C_6-C_5	-0.01	0.01	-2.13
C_3-C_4	1.4016	1.4026	1.392	C_3-C_2-H_{35}	120.81	120.44	119.68	C_2-C_1-C_6-H_{37}	-179.99	-179.97	177.85
C_3-H_{36}	1.0838	1.0834	0.950	C_2-C_3-C_4	117.77	117.63	118.05	O_{33}-C_1-C_6-C_5	180	179.99	178.95
C_4-C_5	1.4202	1.4211	1.415	C_2-C_3-H_{36}	120.70	120.90	120.96	O_{33}-C_1-C_6-H_{37}	0.01	0.01	-1.07
C_4-N_7	1.3726	1.3714	1.379	C_4-C_3-H_{36}	121.53	121.47	120.99	C_1-C_2-C_3-C_4	0.002	0.002	0.73
C_5-C_6	1.4127	1.4139	1.409	C_3-C_4-C_5	121.46	121.48	121.81	C_1-C_2-C_3-H_{36}	-179.99	179.97	-179.25
C_5-C_9	1.4254	1.4243	1.420	C_3-C_4-N_7	130.91	130.78	130.36	H_{35}-C_2-C_3-C_4	-180.00	-179.99	-179.24
C_6-H_{37}	1.0815	1.0813	0.950	C_5-C_4-N_7	107.62	107.74	107.82	H_{35}-C_2-C_3-H_{36}	0.01	-0.03	0.78
N_7-C_8	1.3775	1.3787	1.367	C_4-C_5-C_6	119.88	120.02	119.38	C_2-C_3-C_4-C_5	-0.002	0.02	-2.36
N_7-H_{38}	1.0089	1.0092	0.847	C_4-C_5-C_9	106.86	106.84	106.85	C_2-C_3-C_4-N_7	179.99	179.97	177.60
C_8-C_9	1.3852	1.3869	1.382	C_6-C_5-C_9	133.26	133.14	133.76	H_{36}-C_3-C_4-C_5	179.99	-179.94	177.62
C_8-C_{10}	1.4682	1.4651	1.467	C_1-C_6-C_5	118.25	118.09	118.54	H_{36}-C_3-C_4-N_7	-0.02	0.01	-2.42
C_9-H_{39}	1.0796	1.0792	0.951	C_1-C_6-H_{37}	121.87	121.98	120.74	C_3-C_4-C_5-C_6	-0.003	-0.03	1.76
C_{10}=O_{11}	1.2156	1.2239	1.222	C_5-C_6-H_{37}	119.88	119.93	120.72	C_3-C_4-C_5-C_9	180.00	179.95	-179.05
C_{10}-N_{12}	1.3992	1.3906	1.379	C_4-N_7-C_8	109.39	109.30	108.69	N_7-C_4-C_5-C_6	-179.99	-179.99	-178.20
N_{12}-N_{13}	1.3319	1.3372	1.348	C_4-N_7-H_{38}	128.13	127.13	124.88	N_7-C_4-C_5-C_9	0.01	-0.01	0.99
N_{12}-H_{40}	1.0214	1.0212	0.790	C_8-N_7-H_{38}	122.48	123.57	126.32	C_3-C_4-N_7-C_8	-179.99	-179.95	179.79
N_{13}=C_{14}	1.2932	1.2916	1.295	N_7-C_8-C_9	109.05	109.06	109.80	C_3-C_4-N_7-H_{38}	0.002	0.16	-4.01
C_{14}-C_{15}	1.4980	1.5028	1.505	N_7-C_8-C_{10}	117.36	118.08	119.68	C_5-C_4-N_7-C_8	0.003	0.01	-0.25
C_{14}-C_{18}	1.4562	1.4561	1.455	C_9-C_8-C_{10}	133.59	132.86	130.51	C_5-C_4-N_7-H_{38}	179.99	-179.88	175.95
C_{15}-N_{16}	1.3791	1.3736	1.366	C_5-C_9-C_8	107.07	107.06	106.82	C_4-C_5-C_6-C_1	0.01	0.02	0.52

C_{15}=O_{19}	1.2287	1.2297	1.233	C_5-C_9-H_{39}	126.31	126.15	126.58	C_4-C_5-C_6-H_{37}	179.99	179.99	-179.47
N_{16}-C_{17}	1.4123	1.4117	1.412	C_8-C_9-H_{39}	126.62	126.79	126.60	C_9-C_5-C_6-C_1	-179.99	-179.96	-178.41
N_{16}-C_{20}	1.4568	1.4590	1.470	C_8-C_{10}-O_{11}	122.52	122.42	123.93	C_9-C_5-C_6-H_{37}	-0.01	0.02	1.60
C_{17}-C_{18}	1.4084	1.4080	1.404	C_8-C_{10}-N_{12}	114.02	114.59	111.91	C_4-C_5-C_9-C_8	-0.01	0.01	-1.34
C_{17}=C_{21}	1.3856	1.3858	1.379	O_{11}-C_{10}-N_{12}	123.46	123.00	124.16	C_4-C_5-C_9-H_{39}	-179.99	-179.96	178.61
C_{18}-C_{24}	1.3888	1.3892	1.387	C_{10}-N_{12}-N_{13}	120.21	119.96	122.16	C_6-C_5-C_9-C_8	179.99	179.99	177.60
C_{20}-C_{25}	1.5184	1.5193	1.511	C_{10}-N_{12}-H_{40}	121.23	121.51	120.26	C_6-C_5-C_9-H_{39}	0.01	0.02	-2.36
C_{20}-H_{41}	1.0943	1.0927	0.990	N_{13}-N_{12}-H_{40}	118.56	118.53	117.41	C_4-N_7-C_8-C_9	-0.01	-0.003	-0.62
C_{20}-H_{42}	1.0930	1.0921	0.990	N_{12}-N_{13}-C_{14}	118.11	118.28	114.89	C_4-N_7-C_8-C_{10}	179.91	179.85	178.51
C_{21}-C_{22}	1.3993	1.3994	1.403	N_{13}-C_{14}-C_{15}	127.37	127.54	126.95	H_{38}-N_7-C_8-C_9	-180	179.89	-176.75
C_{21}-H_{43}	1.0821	1.0818	0.950	N_{13}-C_{14}-C_{18}	126.07	126.05	127.18	H_{38}-N_7-C_8-C_{10}	-0.08	-0.26	2.38
C_{22}-C_{23}	1.3936	1.3933	1.380	C_{15}-C_{14}-C_{18}	106.56	106.42	105.87	N_7-C_8-C_9-C_5	0.02	-0.003	1.23
C_{22}-H_{44}	1.0822	1.0821	0.950	C_{14}-C_{15}-N_{16}	106.45	106.51	107.09	N_7-C_8-C_9-H_{39}	179.99	179.97	-178.73
C_{23}-C_{24}	1.3941	1.3936	1.395	C_{14}-C_{15}-O_{19}	127.29	126.81	127.44	C_{10}-C_8-C_9-C_5	-179.89	-179.82	-177.78
C_{23}-Cl_{32}	1.7595	1.7651	1.741	N_{16}-C_{15}-O_{19}	126.26	126.68	125.46	C_{10}-C_8-C_9-H_{39}	0.09	0.15	2.26
C_{24}-H_{45}	1.0821	1.0820	0.951	C_{15}-N_{16}-C_{17}	110.50	110.54	110.16	C_{10}-N_{12}-N_{13}-C_{14}	179.92	-179.92	-178.61
C_{25}-C_{26}	1.3965	1.3976	1.391	C_{15}-N_{16}-C_{20}	123.34	123.82	122.46	H_{40}-N_{12}-N_{13}-C_{14}	0.24	-0.01	-3.36
C_{25}-C_{30}	1.3984	1.3984	1.389	C_{17}-N_{16}-C_{20}	126.06	125.56	127.28	N_{13}-C_{14}-C_{15}-N_{16}	179.74	179.61	179.03
C_{26}-C_{27}	1.3943	1.3945	1.390	N_{16}-C_{17}-C_{18}	109.61	109.74	109.96	N_{13}-C_{14}-C_{15}-O_{19}	-0.3	-0.46	-1.96
C_{26}-H_{46}	1.0853	1.0846	0.950	N_{16}-C_{17}-C_{21}	129.02	128.81	127.95	C_{18}-C_{14}-C_{15}-N_{16}	-0.35	-0.44	-1.47
C_{27}-C_{28}	1.3847	1.3843	1.371	C_{18}-C_{17}-C_{21}	121.37	121.45	122.09	C_{18}-C_{14}-C_{15}-O_{19}	179.62	179.48	177.55
C_{27}-H_{47}	1.0828	1.0828	0.950	C_{14}-C_{18}-C_{17}	106.87	106.78	106.90	N_{13}-C_{14}-C_{18}-C_{17}	-179.91	-179.92	-178.82
C_{28}-C_{29}	1.3870	1.3857	1.369	C_{14}-C_{18}-C_{24}	132.42	132.50	132.49	N_{13}-C_{14}-C_{18}-C_{24}	0.38	0.46	0.45
C_{28}-F_{31}	1.3544	1.3627	1.364	C_{17}-C_{18}-C_{24}	120.71	120.72	120.61	C_{15}-C_{14}-C_{18}-C_{17}	0.17	0.13	1.68
C_{29}-C_{30}	1.3916	1.3932	1.390	N_{16}-C_{20}-C_{25}	114.39	114.23	111.94	C_{15}-C_{14}-C_{18}-C_{24}	-179.54	-179.48	-179.06
C_{29}-H_{48}	1.0828	1.0828	0.950	N_{16}-C_{20}-H_{41}	108.87	108.71	109.19	C_{14}-C_{15}-N_{16}-C_{17}	0.39	0.59	0.69
C_{30}-H_{49}	1.0841	1.0838	0.950	N_{16}-C_{20}-H_{42}	105.50	105.85	109.24	C_{14}-C_{15}-N_{16}-C_{20}	176.90	177.55	177.22
O_{33}-C_{34}	1.4193	1.4271	1.431	C_{25}-C_{20}-H_{41}	109.94	110.14	109.23	O_{19}-C_{15}-N_{16}-C_{17}	-179.57	-179.33	-178.35
C_{34}-H_{50}	1.0888	1.0883	0.980	C_{25}-C_{20}-H_{42}	110.34	110.30	109.25	O_{19}-C_{15}-N_{16}-C_{20}	-3.06	-2.38	-1.82
C_{34}-H_{51}	1.0959	1.0944	0.980	H_{41}-C_{20}-H_{42}	107.51	107.32	107.91	C_{15}-N_{16}-C_{17}-C_{18}	-0.29	-0.53	0.39
C_{34}-H_{52}	1.0959	1.0944	0.980	C_{17}-C_{21}-C_{22}	117.95	117.92	117.24	O_{33}-C_1-C_2-C_3	179.63	179.86	-179.98
O_{19}···H_{40}	1.9742	1.9798									

3.3.2 Natural bond orbital analysis

Natural bond orbital (NBO) analysis produces a chemical picture of (hyper)conjugative interactions from the bonding to anti-bonding orbitals of a compound to understand its intramolecular charge-transfer (ICT) interactions. The results of NBO analysis of compound **5h** are presented in Table 4. The larger E(2) value indicates more intensive interaction between electron donors and acceptors. The interaction of the lone pair of the nitrogen LP(1)N_{16} with π*(C_{15}-O_{19}) yielded an energy value of 52.87 kcal mol^{-1} which is higher than the energy value (39.08 kcal mol^{-1}) of the interaction with the adjacent pair π*(C_{17}-C_{21}) due to the presence of electro negative oxygen in the former pair. Also, the charge transfer interaction between LP(1) N12→π*(C_{10}-O_{11}) exhibited high energy than the interaction LP(1) N12→π*(N_{13}-C_{14}) due to the presence of oxygen atom connected to C_{10}. The lone pair of oxygen LP(2)O_{11} interacts with σ*(C_8-C_{10}) and σ*(C_{10}-N_{12}) with energy values of 16.85 and 27.28 kcal mol^{-1} respectively. While, LP(3)Cl_{32} interacts with σ*(C_{24}-H_{45}) with an energy value 63.25 kcal mol^{-1}. The low electron density (0.0389 e) value of the antibonding orbital N_{12}-H_{40} reveals the more ability to make interactions with the other acceptor motifs. These

results can identify the efficiency of donor and acceptor groups within the compound, which helps the interaction with its target protein.

Table 4. Selective donor acceptor interactions results of compound **5h** based on second-order perturbation theory in Fock matrix.

Donor (i)	ED (i)e	Acceptor (i)	ED[a] (j) e	E(2)[b] (kcal/mol)	E(j)-E(i)[c] (arb.units)	F(i,j)[d] (arb.units)
π (C_4-C_5)	1.57391	π*(C_1-C_6)	0.33686	19.64	0.28	0.068
π (C_4-C_5)	1.57391	π*(C_2-C_3)	0.28170	15.70	0.29	0.062
π (C_4-C_5)	1.57391	π*(C_8-C_9)	0.37198	21.10	0.28	0.069
σ (N_{12}-N_{13})	1.98814	σ*(C_{27}-C_{28})	0.02664	37.92	1.31	0.200
π (C_{17}-C_{21})	1.67568	π*(C_{22}-C_{23})	1.65607	39.95	0.03	0.056
π (C_{18}-C_{24})	1.67839	π*(N_{13}-C_{14})	0.28572	18.87	0.27	0.064
LP(1)N_7	1.59925	π*(C_4-C_5)	0.49729	38.79	0.29	0.097
LP(1)N_7	1.59925	π*(C_8-C_9)	0.37198	36.92	0.28	0.092
LP(2)O_{11}	1.85846	σ*(C_8-C_{10})	0.05788	16.85	0.72	0.100
LP(2)O_{11}	1.85846	σ*(C_{10}-N_{12})	0.08610	27.28	0.63	0.119
LP(1) N_{12}	1.62155	π*(C_{10}-O_{11})	0.30522	42.23	0.30	0.102
LP(1) N_{12}	1.62155	π*(N_{13}-C_{14})	0.28572	42.19	0.28	0.099
LP(1) N_{13}	1.90641	σ*(N_{12}-H_{40})	0.03893	10.73	0.76	0.082
LP(1) N_{13}	1.90641	σ*(C_{14}-C_{18})	0.04195	12.10	0.86	0.092
LP(1) N_{16}	1.64010	π*(C_{15}-O_{19})	0.30742	52.87	0.29	0.112
LP(1) N_{16}	1.64010	π*(C_{17}-C_{21})	0.39926	39.08	0.29	0.096
LP(1) N_{16}	1.64010	π*(C_{27}-C_{28})	0.36353	74.40	0.07	0.065
LP(2) O_{19}	1.84605	σ*(C_{15}-N_{16})	0.08946	27.47	0.68	0.124
LP(1) F_{31}	1.98960	σ*(C_{25}-C_{26})	0.02212	116.92	0.18	0.132
LP(2) F_{31}	1.97242	σ*(C_{24}-H_{45})	0.01369	32.77	0.72	0.138
LP(2) F_{31}	1.97242	σ*(C_{27}-C_{28})	0.02664	51.50	0.77	0.177
LP(3) F_{31}	1.92663	σ*(C_{24}-H_{45})	0.01369	18.83	0.70	0.104
LP(3) F_{31}	1.92663	σ*(C_{26}-C_{27})	0.01334	15.07	0.95	0.109
LP(3) F_{31}	1.92663	σ*(C_{27}-C_{28})	0.02664	55.37	0.74	0.183
LP(2)Cl_{32}	1.96603	σ*(C_{24}-H_{45})	0.01369	14.03	0.58	0.081
LP(2)Cl_{32}	1.96603	σ*(C_{27}-C_{28})	0.02664	19.60	0.63	0.099
LP(2) Cl_{32}	1.96603	π*(C_{27}-C_{28})	0.36353	45.64	0.17	0.086
LP(3) Cl_{32}	1.93242	σ*(C_{24}-H_{45})	0.01369	63.25	0.77	0.200
LP(3) Cl_{32}	1.93242	σ*(C_{27}-C_{28})	0.02664	51.75	0.81	0.185
LP(3) Cl_{32}	1.93242	π*(C_{27}-C_{28})	0.36353	65.56	0.35	0.147
LP(3) Cl_{32}	1.93242	σ*(C_{29}-C_{30})	0.01309	22.34	4.59	0.290
LP(1) O_{33}	1.96348	π*(C_{27}-C_{28})	0.36353	22.38	0.34	0.085
LP(1) O_{33}	1.96348	σ*(C_{29}-C_{30})	0.01309	11.16	4.58	0.203
LP(2) O_{33}	1.84916	π*(C_1-C_6)	0.33686	27.20	0.34	0.091
LP(2) O_{33}	1.84916	π*(C_{27}-C_{28})	0.36353	34.67	0.09	0.051

[a]Electron density; [b]Energy of stabilization interactions; [c]Energy difference between donor and acceptor i and j NBO orbital; [d]Fock matrix element between i and j NBO orbital.

3.3.3 Natural population analysis (NPA)

The atomic charge of compound **5h** was calculated by natural population analysis (NPA). It is an effective method to calculate the atomic charges within the molecule. The plot of charge

distribution is shown in Figure 3. The C_{15} (0.669 e) and C_{10} (0.646 e) atoms showed more positive charge than the other carbon atoms due to the presence of electronegative oxygen atom directly attached to them. Whereas, The C_8 (0.032 e), C_{14} (0.100 e), and C_{17} (0.188 e) atoms showed positive charge because of their bonding with nitrogen atoms. On the other hand, the other carbon atoms manifested negative charges. The N_7 (-0.532 e) is more negative than the other nitrogen atoms N_{16} (-0.482 e), N_{12} (-0.389 e) and N_{13} (-0.204 e). All hydrogen atoms displayed positive charges in which H_{38} (0.446 e) and H_{40} (0.378 e) are the most positive owing to their direct attachment to nitrogen atoms.

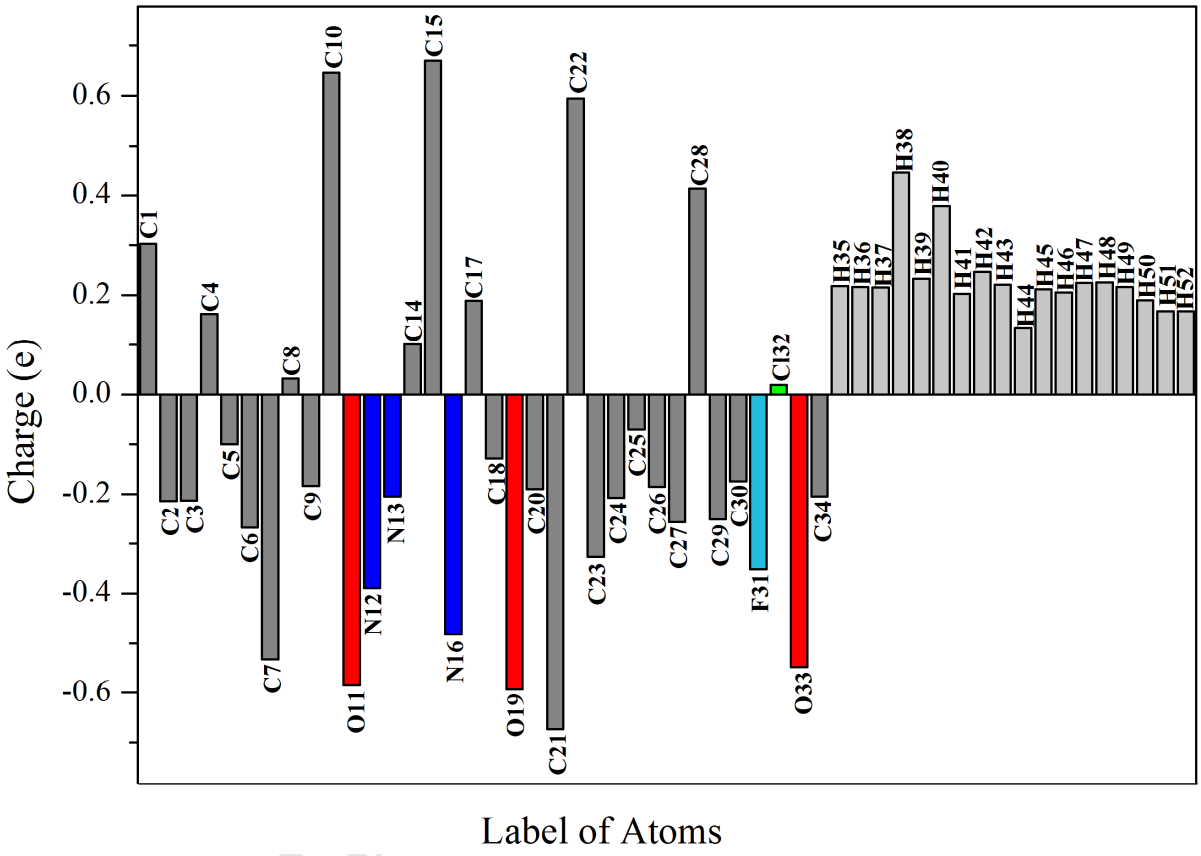

Figure 3. Charge distribution chart for compound **5h** according to the natural population analysis.

3.3.4 Frontier molecular orbital analysis

The chemical reactivity and kinetic stability of the molecules are determined by the highest occupied molecular orbital (HOMO) and lowest unoccupied molecular orbital (LUMO).The former represents the ability to donate an electron while the latter represents the ability to accept an electron [45]. A molecule is more reactive for a small HOMO-LUMO energy gap [46]. The energies have been calculated by B3LYP/6-311++G(d,p) methods and are depicted in the Figure 4. The energy gap between HOMO and LUMO of the test compound **5h** is 2.79

eV. The lowering of HOMO-LUMO energy gap reveals the possibility of charge transfer interaction within the molecule.

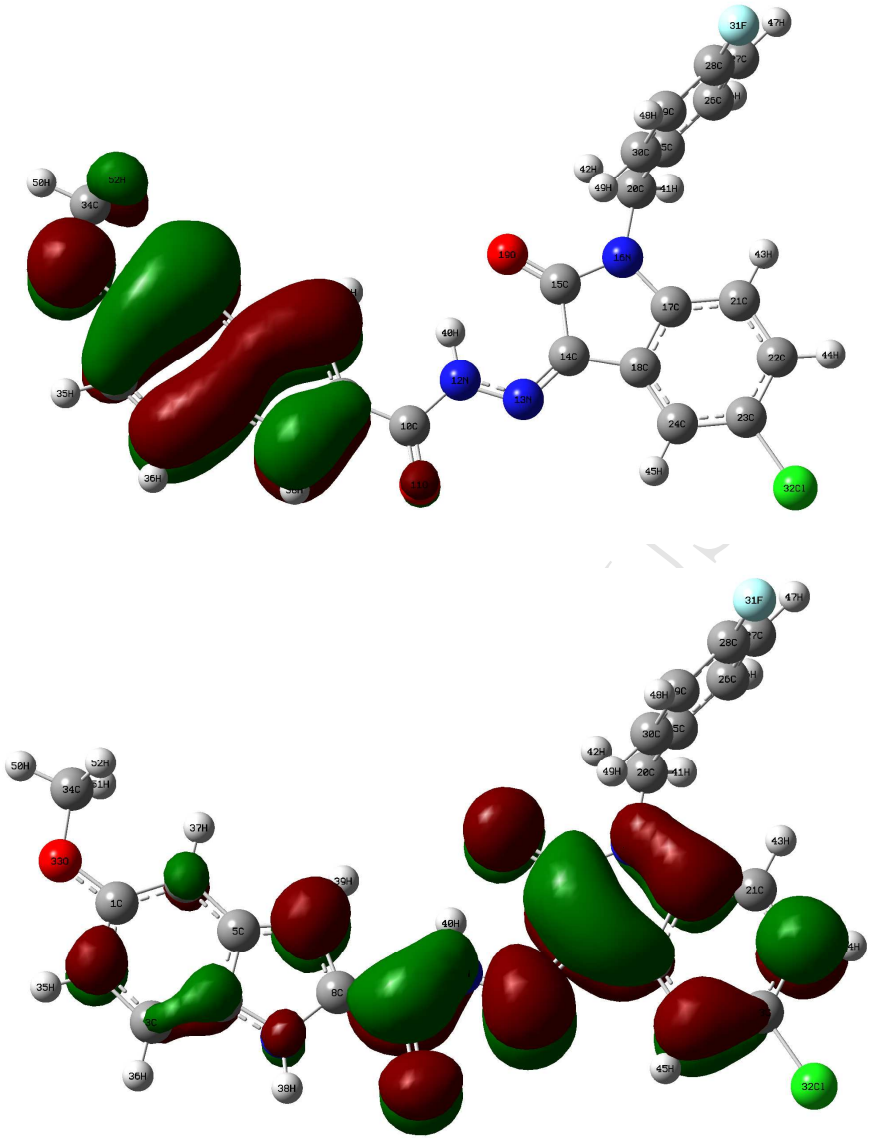

Figure 4. HOMO (upper) and LUMO (lower) energy plots of compound **5h**.

3.3.5. Vibrational analysis

The vibrational spectral analysis of compound **5h** was carried out on the basis of the characteristic vibrations of indole ring, phenyl ring, methoxy group, as well as methylene and carbonyl groups. The observed and simulated FT-IR and FT-Raman spectra are shown in Figures 5 and 6, respectively. The computed and experimental wavenumbers as well as their assignments with PED were presented in Table 5.

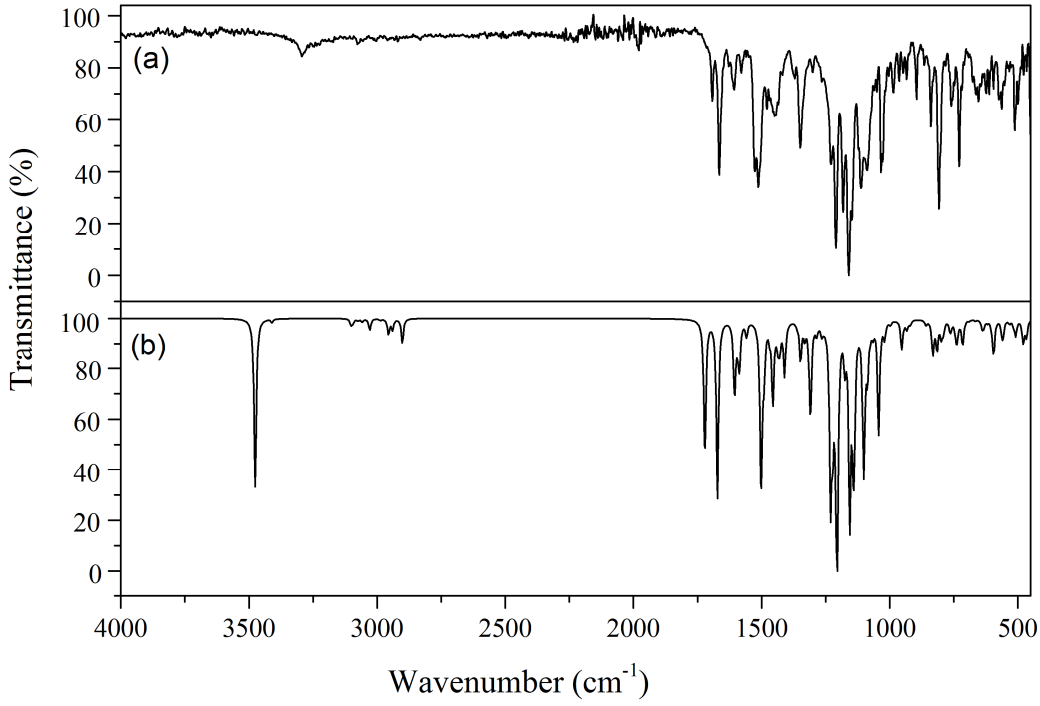

Figure 5. (a) Experimental (b) Simulated infrared spectra of compound **5h** in the region 4000-500 cm^{-1}.

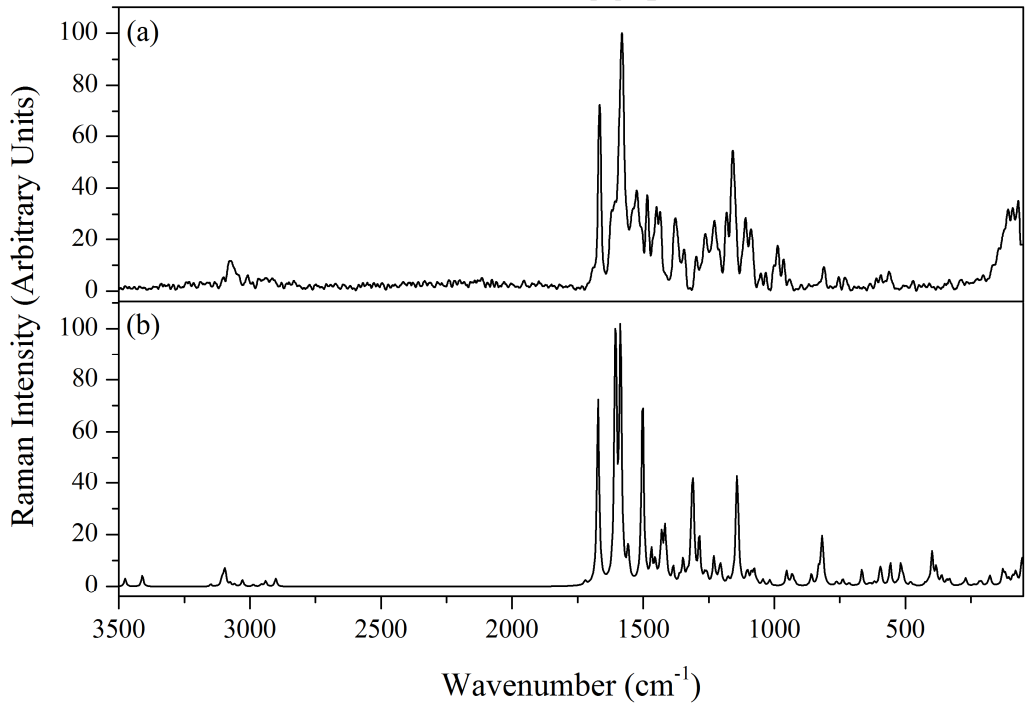

Figure 6. (a) Experimental (b) Simulated Raman spectra of compound **5h** in the region 3500-50 cm^{-1}.

Table 5. Tentative vibrational assignments of compound **5h** predicted based on PED analysis.

Calculated Wavenumber (cm^{-1})		Experimental Wavenumber (cm^{-1})		Assignment with PED (%)
Unscaled	Scaled	IR	Raman	
3593	3476	3293 vw		ν N_7-H_{38}(99)
3206	3101		3101 w	ν C_{24}-H_{45}(98)
3181	3077		3076 w	ν C_2-H_{35}(25), ν C_3-H_{36}(75)
3162	3058	3057 w	3043 w	ν C_{26}-H_{46}(96)
3131	3029		3008 w	ν C_{34}-H_{50}(92)
3040	2940		2941w	ν C_{34}-H_{51}(76)
3031	2933			ν_{as} C_{20}-H_{41}(45)
1729	1672	1665 m	1666 s	ν O_{11}=C_{10}(77)
1662	1607	1608 w		νC_2=C_3(16), ν C_1=C_6(17),ν C_3-C_4(13)
1636	1583	1579 vw	1581vs	ν C_{27}=C_{28}(32), ν C_{25}-C_{26}(20)
1612	1559	1560 vw		ν C_{22}-C_{23}(16), ν C_{17}-C_{18}(19)
1553	1502	1509 m	1525 m	ν C_8-C_9(20),ν C_3-C_4(10)
1541	1490		1484 m	ν C-H ph
1518	1469	1479 vw		sci H_{41}-C_{20}-H_{42}(12)
1503	1454		1449 m	ν_{as} C_{34}-H_{52}(63)
1490	1441	1445 w		$\nu_{as}$$C_{34}$-$H_{51}$(76)
1484	1436		1436 m	d C_{34}-H_{51}-H_{52}-H_{50}(31)
1394	1348	1349 m	1344 w	ν C_2=C_3(13), ν C_1=C_6(17), ν C_5-C_6(11)
1331	1287		1297 w	β H_{46}-C_{26}-C_{27}(23),H_{49}-C_{30}-C_{29}(22)
1273	1231	1229 w	1228 m	ν N_7-C_4(12)
1251	1210	1210 m		ρ CH_3 (38) methoxy
1244	1203	1204 s		ν F_{31}-C_{28}(45)Ph
1218	1178	1181 m	1182 m	βC-H, H_{46}-C_{26}-C_{27}(11)
1195	1156	1159 s	1158 m	ν O33-C34 (59)
1143	1106	1112 m	1110 m	ρ –O-CH_3 (42)
1124	1087	1088 w	1089 m	β H_{47}-C_{27}-C_{26}(18),H_{48}-C_{29}-C_{30}(15),H_{46}-C_{26}-C_{27}(11),H_{49}-C_{30}-C_{29}(10)
1101	1065	1050 vw	1052 w	βC-H,H_{48}-C_{29}-C_{30}(27)Ph
1055	1020	1024 w		ρ –O-CH_3 (15)
1031	998	985 w	987 w	γ C_{28}-C_{29}-C_{30}-H_{49}(43),C_{27}-C_{28}-C_{29}-H_{48}(16)Ph
977	945	948 vw	942 w	γ C_{26}-C_{25}-C_{27}-H_{46}(19), H_{48}-C_{29}-C_{30}-H_{49}(59)Ph
860	832	839 vw		b Ph
847	819	820 m		b Ph
843	815		811w	b Ph
830	803	808 m		b Ph
784	759	759 vw	754 w	ν C23-Cl32(41)
755	730	729 w	731w	ρ –CH_2 (23)
581	562	563 vw	562 w	d -OCH_3(18)
526	508	512 w		d -OCH_3(22)
494	478	477 vw		d -OCH_3(28)
482	466	466 vw		d -OCH_3(19)
439	424	422w		d -OCH_3(20)
218	210		203 w	τ -OCH_3(26)

ν-stretching; ν_{as}-asymmetric stretching; δ-bending; τ-torsion; β-in-plane bending; γ-out-of-plane bending; sci-scissoring; ρ-rocking; d-deformation; b-ring breathing; vs-very strong; s-strong; m-medium; vw-very weak; w-weak; ph: phenyl ring.

3.3.5.1. Indole ring vibrations

In solution, the N-H stretching vibration occurs near 3400 cm^{-1} while in solid state, the frequency shifts towards lower values [47]. A band was observed due to the N-H stretching vibration in the IR spectrum of compound **5h** at 3293 cm^{-1}. A band occurred in the Raman spectrum of compound **5h** at 3076 cm^{-1} which was assigned to C-H stretching of indole. The indole ring C-C stretching vibrations are expected to be in the region 1625 cm^{-1} to 1300 cm^{-1} [47] and it was observed in the IR spectrum of compound **5h** at 1608 cm^{-1}. The C-N stretching mode is reported at 1244 and 1227cm^{-1} for indole [48] which occurred at 1229 and 1228 cm^{-1} in the IR and Raman spectra of compound **5h**, respectively.

3.3.5.2. Phenyl ring

The C-H stretching bands occur in the region of 3080-3010 cm^{-1}. The weak bands observed at 3057 and 3043 cm^{-1} in the IR and Raman spectra, respectively, of compound **5h** correspond to the C-H stretching mode. The ring C-C stretching vibrations occur in the region of 1625-1430 cm^{-1} [47]. A weak band was observed at 1579 cm^{-1} in the IR spectrum of compound **5h** and a very strong band at 1581 cm^{-1} in its Raman spectrum which were assigned for the C-C stretching mode. The fluorine atom attached to an aromatic ring gives absorption band in the region of 1270-1100 cm^{-1} [49] which was noted as a strong band at 1204 cm^{-1} in the IR spectrum of compound **5h**. The stretching modes for *para* substituted fluoro phenyl ring are expected to be in the range 1620-1280 cm^{-1} [50]. A medium band was observed in the Raman spectrum of compound **5h** at 1484 cm^{-1} which was assigned to the *para* substituted fluoro phenyl ring.

3.3.5.3. Methoxy group vibrations

The methoxy asymmetric and symmetric stretching bands occur around 2960 and 2846 cm^{-1}, respectively. A weak band was observed at 2941 cm^{-1} in the Raman spectrum of compound **5h** which was assigned to methoxy group symmetric stretching vibration. The asymmetric C-H bending vibrations appear in the region of 1470-1440 cm^{-1} [51]. These vibrations were noted as a medium intense band at 1449 cm^{-1} in the Raman spectrum of compound **5h** and at 1445 cm^{-1} in its IR spectrum. The strong band at 1159 cm^{-1} in the IR spectrum of compound **5h** and a medium band at 1158 cm^{-1} in its Raman spectrum were assigned to the C-O stretching [52].

3.3.5.4. Methylene vibrations

Asymmetric stretching vibration for methylene group appears about 2930 cm^{-1} [49]. A weak band was observed at 2941 cm^{-1} in the IR spectrum of compound **5h** which was assigned for this mode. Scissoring and rocking vibrations of methylene occur in the region of 1480-1440

cm^{-1} and 730-710 cm^{-1}, respectively [53]. The observed weak intensity band at 1479 cm^{-1} in the IR spectrum of compound **5h** corresponds to its scissoring vibration. While, the noticed bands of weak intensity at 729 and 731 cm^{-1} in the IR and Raman spectra of compound **5h**, respectively, were assigned for its rocking vibrations.

3.2.5.5. Carbonyl vibration

The C=O stretching vibrations appear as intense bands between 1870 and 1540 cm^{-1}. The position of these bands is determined by the neighbouring substituents, conjugations and hydrogen bonding [54]. Strong and medium bands were observed at 1666 and 1665 cm^{-1} in the Raman and IR spectra of compound **5h** which were assigned to its C=O stretching mode.

3.3.5.6. Chloro-Indole vibrations

The chloro-indole ring shows strong absorption bands in the range of 760-505 cm^{-1} for C-Cl stretching vibration. A shift might occur in the upper limit to 840 cm^{-1}, if there is a vibrational coupling with other vibrations [47]. Compound **5h** manifested a stretching absorption band in its IR and Raman spectra at 759 and 754 cm^{-1}, respectively.

3.3.6. Molecular docking studies

Molecular docking was performed using AutoDock 4.2 software interfaced with AutoDock Tools v1.5.6rc3 based on Lamarckian Genetic algorithm [42]. Compound **5h** was energy minimized using Gaussian′09 program package at DFT level. The *C. albicans* target protein (PDB code: 1IYL) was selected for the present investigation. Its XRD structural coordinates were downloaded from research collaboratory for structural bioinformatics (RCSB) protein data bank, with a resolution of 3.2 Å. The rigid docking of flexible ligand was carried out into the target protein by AutoDockTools program. Partial atomic charges were added using Kollman's method. The grid box was set as 90 x 90 x 90 points with spacing 0.913 Å over the target protein binding pocket. Visualization (Figure 7) was performed with PyMOL v1.2r1 program [55] and it manifested that the amidic NH of compound **5h** interacts with the amino acid residue Tyr354 of the target protein. The protein-ligand complex has been stabilized by the formation of this N-H···O hydrogen bond interaction. This hydrogen bond interaction (ligand (N-H) : protein (O)) has been predicted by NBO analysis based on the low electron occupancy on the N-H orbital. The binding energy of the best docked conformation of compound **5h** is -7.79 $kcal.mol^{-1}$ with estimated inhibition constant of 1.44 µM and it has been selected from 100 conformations (100 GA run). Moreover, docking of the antifungal drug, fluconazole, into the target protein (1IYL) in a similar manner like **5h**, gave protein-ligand binding energy of -4.99 $kcal.mol^{-1}$ indicating the possible anti-*Candida* activity of

compound **5h**. The docking results showed the possible binding mode of compound **5h** with its target protein (1IYL) and predicted its anti-*C. albicans* activity.

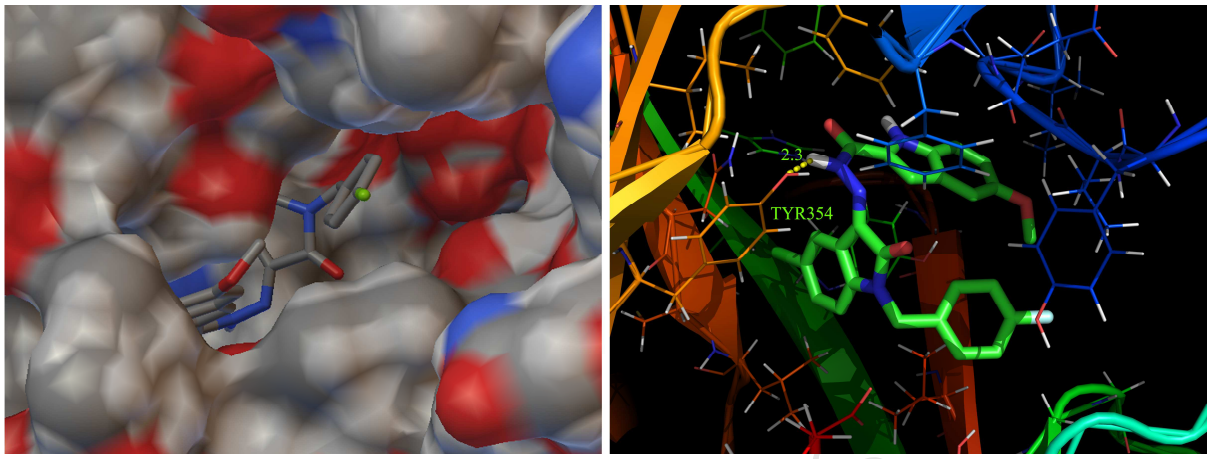

Figure 7. Binding pose of compound **5h** with its target protein.

4. Conclusion

Nine indole-isatin molecular hybrids **5a-i** have been successfully prepared and characterized using various spectroscopic techniques. The title compounds **5a-i** were estimated for their antimicrobial activity using DIZ and MIC assays. Compound **5c** emerged as the most active congener towards *Ps. aeruginosa* with MIC value of 3.9 µg mL^{-1}. Whereas, compound **5i** is the most active congener against *A. niger* and compounds **5b** and **5h** are the most active and equipotent towards *P. notatum* with MIC value of 7.8 µg mL^{-1}. The vibrational spectroscopic analysis of *N'*-[(3*Z*)-5-chloro-1-(4-fluorobenzyl)-2-oxo-1,2-dihydro-3*H*-indol-3-ylidene]-5-methoxy-1*H*-indole-2-carbohydrazide (**5h**) was performed experimentally using FT-IR and FT-Raman and theoretically by DFT/B3LYP method. The optimized geometric parameters, vibrational harmonic frequencies, PED assignments and molecular orbital energies of the compound **5h** have been calculated by DFT/B3LYP method with 6-311++G(d,p) basis set. The theoretical optimized geometric parameters and vibrational frequencies are compared with the experimental data and their level of correlation is fairly good. The detailed PED analysis of compound **5h** showed a good agreement with the experimental data. The charge-transfer occurring within the molecule can be understood by its HOMO and LUMO energy values. Molecular docking study manifested the possible binding mode of compound **5h** with its fungal target protein. The results of the current exploration could be harnessed to develop new bioactive indole-based antimicrobial molecules.

Supplementary material

Figure S1 and the NMR spectra of the synthesized compounds **5a-i** are provided as supplementary materials.

Acknowledgements

The authors would like to extend their sincere appreciation to the Deanship of Scientific Research at King Saud University for its funding of this research through the Research Group Project no. RGP-196.

References

[1] A. Srivastava, S. Pandeya, Indole a versatile nucleus in pharmaceutical field, Int. J. Curr. Pharm. Rev. Res. 4 (2011) 5-8.

[2] S. Biswal, U. Sahoo, S. Sethy, H. Kumar, M. Banerjee, Indole: the molecule of diverse biological activities, Asian J. Pharm. Clin. Res. 5 (1) (2012) 1-6.

[3] D.G. Giménez, E.G. Prado, T.S. Rodríguez, A.F. Arche, R. De la Puerta, Cytotoxic effect of the pentacyclic oxindole alkaloid mitraphylline isolated from Uncaria tomentosa bark on human Ewing's sarcoma and breast cancer cell lines, Planta medica 76 (02) (2010) 133-136.

[4] S.R. Wedge, J. Kendrew, L.F. Hennequin, P.J. Valentine, S.T. Barry, S.R. Brave, N.R. Smith, N.H. James, M. Dukes, J.O. Curwen, R. Chester, J.A. Jackson, S.J. Boffey, L.L. Kilburn, S. Barnett, G.H. Richmond, P.F. Wadsworth, M. Walker, A.L. Bigley, S.T. Taylor, L. Cooper, S. Beck, J.M. Jurgensmeier, D.J. Ogilvie, AZD2171: a highly potent, orally bioavailable, vascular endothelial growth factor receptor-2 tyrosine kinase inhibitor for the treatment of cancer, Cancer Res. 65 (10) (2005) 4389-400.

[5] N.K. Kaushik, N. Kaushik, P. Attri, N. Kumar, C.H. Kim, A.K. Verma, E.H. Choi, Biomedical importance of indoles, Molecules 18 (6) (2013) 6620-6662.

[6] M.I. Attia, P.A. Witt-Enderby, J. Julius, Synthesis and pharmacological evaluation of pentacyclic 6a,7-dihydrodiindole and 2,3-dihydrodiindole derivatives as novel melatoninergic ligands, Bioorg. Med. Chem. 16 (16) (2008) 7654-7661.

[7] C. Markl, M.I. Attia, J. Julius, S. Sethi, P.A. Witt-Enderby, D.P. Zlotos, Synthesis and pharmacological evaluation of 1,2,3,4-tetrahydropyrazino[1,2-a]indole and 2-[(phenylmethylamino)methyl]-1*H*-indole analogues as novel melatoninergic ligands, Bioorg. Med. Chem. 17 (13) (2009) 4583-4594.

[8] C. Markl, W.P. Clafshenkel, M.I. Attia, S. Sethi, P.A. Witt-Enderby, D.P. Zlotos, N-Acetyl-5-arylalkoxytryptamine analogs: probing the melatonin receptors for MT_1 -selectivity, Arch. Pharm. (Weinheim) 344 (10) (2011) 666-674.

[9] S.N. Pandeya, S. Smitha, M. Jyoti, S.K. Sridhar, Biological activities of isatin and its derivatives, Acta Pharm. 55 (1) (2005) 27-46.

[10] S.N. Pandeya, P. Yogeeswari, D.S. Ram, G. Nath, Synthesis and antimicrobial activity of *N*-Mannich bases of 3-[*N*'-sulphadoximino]isatin and its methyl derivative, Boll. Chim. Farm. 137 (8) (1998) 321-324.

[11] S.N. Pandeya, D. Sriram, G. Nath, E. De Clercq, Synthesis, antibacterial, antifungal and anti-HIV evaluation of Schiff and Mannich bases of isatin derivatives with 3-amino-2-methylmercapto quinazolin-4(3H)-one, Pharm. Acta Helv. 74 (1) (1999) 11-17.

[12] S.N. Pandeya, D. Sriram, G. Nath, E. DeClercq, Synthesis, antibacterial, antifungal and anti-HIV activities of Schiff and Mannich bases derived from isatin derivatives and *N*-[4-(4'-chlorophenyl)thiazol-2-yl]thiosemicarbazide, Eur. J. Pharm. Sci. 9 (1) (1999) 25-31.

[13] S.K. Bhattacharya, A. Chakrabarti, Dose-related proconvulsant and anticonvulsant activity of isatin, a putative biological factor, in rats, Indian J. Exp. Biol. 36 (1) (1998) 118-121.

[14] H. Zou, L. Zhang, J. Ouyang, M.A. Giulianotti, Y. Yu, Synthesis and biological evaluation of 2-indolinone derivatives as potential antitumor agents, Eur. J. Med. Chem. 46 (12) (2011) 5970-5977.

[15] A. Kamal, Y.V. Srikanth, M.N. Khan, T.B. Shaik, M. Ashraf, Synthesis of 3,3-diindolyl oxyindoles efficiently catalysed by FeCl3 and their in vitro evaluation for anticancer activity, Bioorg. Med. Chem. Lett. 20 (17) (2010) 5229-5231.

[16] K.L. Vine, V. Indira Chandran, J.M. Locke, L. Matesic, J. Lee, D. Skropeta, J.B. Bremner, M. Ranson, Targeting urokinase and the transferrin receptor with novel, anti-mitotic *N*-alkylisatin cytotoxin conjugates causes selective cancer cell death and reduces tumor growth, Curr. Cancer Drug Targets 12 (1) (2012) 64-73.

[17] V.R. Solomon, C. Hu, H. Lee, Hybrid pharmacophore design and synthesis of isatin-benzothiazole analogs for their anti-breast cancer activity, Bioorg. Med. Chem. 17 (21) (2009) 7585-7592.

[18] A.T. Taher, N.A. Khalil, E.M. Ahmed, Synthesis of novel isatin-thiazoline and isatin-benzimidazole conjugates as anti-breast cancer agents, Arch. Pharm. Res. 34 (10) (2011) 1615-1621.

[19] L.A. McAllister, R.A. McCormick, K.M. James, S. Brand, N. Willetts, D.J. Procter, A Fluorous, Pummerer cyclative-capture strategy for the synthesis of *N*-heterocycles, Chem.-A Eur. J. 13 (4) (2007) 1032-1046.

[20] C.-T. Chiou, W.-C. Lee, J.-H. Liao, J.-J. Cheng, L.-C. Lin, C.-Y. Chen, J.-S. Song, M.-H. Wu, K.-S. Shia, W.-T. Li, Synthesis and evaluation of 3-ylideneoxindole acetamides as potent anticancer agents, Eur. J. Med. Chem. 98 (2015) 1-12.

[21] A. Beauchard, Y. Ferandin, S. Frère, O. Lozach, M. Blairvacq, L. Meijer, V. Thiéry, T. Besson, Synthesis of novel 5-substituted indirubins as protein kinases inhibitors, Bioorg. Med. Chem. 14 (18) (2006) 6434-6443.

[22] M.S. Almutairi, S. Xavier, M. Sathish, H.A. Ghabbour, S. Sebastian, S. Periandy, R.I. Al-Wabli, M.I. Attia, Spectroscopic (FT-IR, FT-Raman, UV, ^{1}H and ^{13}C NMR) profiling and computational studies on methyl 5-methoxy-1*H*-indole-2-carboxylate: A potential precursor to biologically active molecules, J. Mol. Struct. 1133 (2017) 199-210.

[23] D.H. Dethe, G.M. Murhade, Diversity-Oriented Synthesis of Calothrixins and Ellipticines, Eur. J. Org. Chem. 2014 (31) (2014) 6953-6962.

[24] L. Garcia, "Biochemical tests for the identification of aerobic bacteria," in clinical microbiology procedures, 3rd ed., pp. 503-642, ASM Press, Washington, DC, 2004.

[25] L.S. Garcia, Clinical microbiology procedures handbook, American Society for Microbiology Press, Washington, DC, 2010.

[26] Clinical and Laboratory Standards Institute (CLSI), abbreviated identification of bacteria and yeast, 2nd ed. CLSI document M35-A2, Clinical and Laboratory Standards Institute (CLSI),Wayne, PA, 2008.

[27] National Committee for Clinical Laboratory Standards, Methods for Determining Bactericidal Activity of antimicrobial agents; approved guideline, NCCLS document M26-A, Wayne, PA, 1999.

[28] Clinical and Laboratory Standards Institute (CLSI), Performance standards for antimicrobial susceptibility testing, "Twenty-First Informational Supplement. M100-S21, vol. 31, no. 1, 2011.

[29] Clinical Laboratory Standards Institute (CLSI), "Methods for dilution antimicrobial susceptibility tests for bacteria that grow aerobically," CLSI document M07-A10, Wayne, PA, 2015.

[30] Clinical and Laboratory Standards Institute (2008a) Reference method for broth dilution antifungal susceptibility testing of yeasts; approved standard-third edition; CLSI document M27-A3. Clinical and Laboratory Standards Institute, Wayne, PA.

[31] Clinical and Laboratory Standards Institute (2008b) Reference method for broth dilution antifungal susceptibility testing of filamentous fungi; approved standard CLSI document M38-A2. Clinical and Laboratory Standards Institute, Wayne, PA.

[32] National Committee Clinical Laboratory Standards, Performance standards for antimicrobial disk susceptibility tests. M100-S21, vol. 31, no. 1, 2011.

[33] Clinical and Laboratory Standards Institute (CLSI), Performance standards for antimicrobial disk susceptibility tests, approved standards, 12th ed. M02-A12, CLSI document, Wayne, PA, 2015.

[34] C. Stadtländer, Scanning electron microscopy and transmission electron microscopy of mollicutes: challenges and opportunities, Mod. Res. Edu. Topics Microsc. 1 (2007) 122-131.

[35] R.A. Gaussian09, 1, MJ Frisch, GW Trucks, HB Schlegel, GE Scuseria, MA Robb, JR Cheeseman, G. Scalmani, V. Barone, B. Mennucci, GA Petersson et al., Gaussian, Inc., Wallingford CT (2009).

[36] A.D. Becke, Density-functional thermochemistry. III. The role of exact exchange, J. Chem. Phys. 98 (7) (1993) 5648-5652.

[37] A.D. Becke, Density-functional exchange-energy approximation with correct asymptotic behavior, Phys. Rev. A Gen. Phys. 38 (6) (1988) 3098-3100.

[38] C. Lee, W. Yang, R.G. Parr, Development of the Colle-Salvetti correlation-energy formula into a functional of the electron density, Phys. Rev. B Condens Matter 37.(2) (1988) 785-789.

[39] A.P. Scott, L. Radom, Harmonic vibrational frequencies: an evaluation of Hartree-Fock, Møller-Plesset, quadratic configuration interaction, density functional theory, and semiempirical scale factors, J. Phys. Chem. 100 (41) (1996) 16502-16513.

[40] M.H. Jamroz, Vibrational energy distribution analysis (VEDA): scopes and limitations, Spectrochim. Acta A Mol. Biomol. Spectrosc. 114 (2013) 220-30.

[41] E. Glendening, A. Reed, J. Carpenter, F. Weinhold, NBO v 3.1; Theoretical Chemistry Institute and Department of Chemistry, University of Wisconsin, Madison, WI, 1998.

[42] G.M. Morris, R. Huey, W. Lindstrom, M.F. Sanner, R.K. Belew, D.S. Goodsell, A.J. Olson, AutoDock4 and AutoDockTools4: Automated docking with selective receptor flexibility, J. Comput. Chem. 30 (16) (2009) 2785-2791.

[43] M.I. Attia, J. Julius, P.A. Witt-Enderby, D.P. Zlotos, Synthesis and pharmacological evaluation of 6a, 7-dihydro-6H, 13*H*-pyrazino [1, 2-a; 4, 5-a′] diindole analogs as melatonin receptor ligands, Tetrahedron 63 (3) (2007) 754-760.

[44] N.G. Haress, H.A. Ghabbour, M.S. Almutairi, H.-K. Fun, M.I. Attia, Crystal structure of 5-methoxy-*N*'-[(3*Z*)-5-chloro-1-(4-fluorobenzyl)-2-oxo-1,2-dihydro-3*H*-indol-3-ylidene]-1*H*-indole-2-carbohydrazide-DMSO (1/1), $C_{25}H_{18}ClFN_4O_3 .C_2H_6OS$ Z. Krist. New Crys. Struct. 231 (4) (2016) 1021–1023.

[45] M. Karabacak, E. Kose, A. Atac, M. Ali Cipiloglu, M. Kurt, Molecular structure investigation and spectroscopic studies on 2,3-difluorophenylboronic acid: a combined experimental and theoretical analysis, Spectrochim. Acta A Mol. Biomol. Spectrosc. 97 (2012) 892-908.

[46] K. Chaitanya, Molecular structure, vibrational spectroscopic (FT-IR, FT-Raman), UV-vis spectra, first order hyperpolarizability, NBO analysis, HOMO and LUMO analysis, thermodynamic properties of benzophenone 2,4-dicarboxylic acid by ab initio HF and density functional method, Spectrochim. Acta A Mol. Biomol. Spectrosc. 86 (2012) 159-173.

[47] M. Tammer, G. Sokrates: Infrared and Raman characteristic group frequencies: tables and charts, Colloid Polym. Sci. 283 (2) (2004) 235-235.

[48] S. Bayar, S. Saglam, H.F. Ustundag, Experimental and theoretical studies of the vibrational spectrum of 5-hydroxytryptamine, J. Mol. Struct.: THEOCHEM 726 (1) (2005) 225-232.

[49] Y.S. Mary, H.T. Varghese, C.Y. Panicker, T. Ertan, I. Yildiz, O. Temiz-Arpaci, Vibrational spectroscopic studies and ab initio calculations of 5-nitro-2-(*p*-fluorophenyl)benzoxazole, Spectrochim. Acta A Mol. Biomol. Spectrosc. 71 (2) (2008) 566-571.

[50] G. Varsányi, Assignments for vibrational spectra of seven hundred benzene derivatives, Halsted Press1974.

[51] B.H. Stuart, Organic molecules, Infrared spectroscopy: Fundamentals and applications (2004) 71-93.

[52] D. Lin-Vien, N.B. Colthup, W.G. Fateley, J.G. Grasselli, The handbook of infrared and Raman characteristic frequencies of organic molecules, Elsevier 1991.

[53] B. Smith, Infrared Spectral Interpretation - A Systematic Approach CRC Press LLC Boca Raton, FL (1999).

[54] R.M. Silverstein, F.X. Webster, D.J. Kiemle, D.L. Bryce, Spectrometric identification of organic compounds, John Wiley & Sons 2014.

[55] W.L. DeLano, The PyMOL molecular graphics system, (2002).

- Synthesis and spectroscopic characterization of new indole-isatin hyprids **5a-i** are reported.
- Antimicrobial activities of the title molecules **5a-i** were assessed.
- FT-IR, FT-Raman, HOMO-LUMO and molecular docking were performed for compound **5h**.
- The geometrical parameters of compound **5h** are in agreement with its XRD data.